







# The Slack Channel Regulates Anxiety-Like Behaviors via Basolateral Amygdala Glutamatergic Projections to Ventral Hippocampus

 Qi Zhang,<sup>1,2,3\*</sup> Shun-Heng Gao,<sup>1,2\*</sup> Zhong-Shan Shen,<sup>1,2,3\*</sup> Yun Wang,<sup>1,2\*</sup>  Su-Wan Hu,<sup>1,2,3\*</sup> Guang-Bing Duan,<sup>1,2</sup> Ye Liu,<sup>1,2,3</sup> Dan-Ya Zhong,<sup>1,2,3</sup> Jing Liu,<sup>1,2,3,4</sup>  Meng-Han Sun,<sup>1,2,3</sup> Xin Zhang,<sup>1,2,3</sup> Tian-Yu Cao,<sup>1,2,3</sup>  Jun-Li Cao,<sup>1,2,3,5</sup>  Qiong-Yao Tang,<sup>1,2,3</sup> and  Zhe Zhang<sup>1,2,3</sup>

<sup>1</sup>Jiangsu Province Key Laboratory of Anesthesiology, Xuzhou Medical University, Xuzhou, Jiangsu 221004, China, <sup>2</sup>Jiangsu Province Key Laboratory of Anesthesia and Analgesia Application Technology, Xuzhou Medical University, Xuzhou, Jiangsu 221004, China, <sup>3</sup>National Medical Products Administration Key Laboratory for Research and Evaluation of Narcotic and Psychotropic Drugs, Xuzhou Medical University, Xuzhou, Jiangsu 221004, China, <sup>4</sup>Department of Cell Biology and neurobiology, Life Sciences College, Xuzhou Medical University, Xuzhou, Jiangsu 221004, China, and <sup>5</sup>Department of Anesthesiology, The Affiliated Hospital of Xuzhou Medical University, Xuzhou, Jiangsu 221002, China

Anxiety disorders are a series of mental disorders characterized by anxiety and fear, but the molecular basis of these disorders remains unclear. In the present study, we find that the global *Slack KO* male mice exhibit anxious behaviors, whereas the *Slack Y777H* male mice manifest anxiolytic behaviors. The expression of Slack channels is rich in basolateral amygdala (BLA) glutamatergic neurons and downregulated in chronic corticosterone-treated mice. In addition, electrophysiological data show enhanced excitability of BLA glutamatergic neurons in the *Slack KO* mice and decreased excitability of these neurons in the *Slack Y777H* mice. Furthermore, the Slack channel deletion in BLA glutamatergic neurons is sufficient to result in enhanced avoidance behaviors, whereas *Kcnt1* gene expression in the BLA or BLA–ventral hippocampus (vHPC) glutamatergic projections reverses anxious behaviors of the *Slack KO* mice. Our study identifies the role of the Slack channel in controlling anxious behaviors by decreasing the excitability of BLA–vHPC glutamatergic projections, providing a potential target for anxiolytic therapies.

**Key words:** anxiety; basolateral amygdala; corticosterone; Slack channel; ventral hippocampus

## Significance Statement

Anxiety disorders are a series of mental disorders characterized by anxiety and fear, but the molecular basis of these disorders remains unclear. Here, we examined the behaviors of loss- and gain-of-function of Slack channel mice in elevated plus maze and open field tests and found the anxiolytic role of the Slack channel. By altering the Slack channel expression in the specific neuronal circuit, we demonstrated that the Slack channel played its anxiolytic role by decreasing the excitability of BLA–vHPC glutamatergic projections. Our data reveal the role of the Slack channel in the regulation of anxiety, which may provide a potential molecular target for anxiolytic therapies.

Received Oct. 7, 2021; revised Jan. 5, 2022; accepted Feb. 8, 2022.

Author contributions: Q.Z., S.-W.H., J.-L.C., Q.-Y.T., and Z.Z. designed research; Q.Z., S.-H.G., Z.-S.S., Y.W., S.-W.H., G.-B.D., Y.L., D.-Y.Z., J.L., M.-H.S., X.Z., and T.-Y.C. performed research; Q.Z. and Y.L. analyzed data; Q.Z. and Z.Z. wrote the paper.

This work was supported by The Important Project of Natural Science in Colleges and Universities in Jiangsu Province to Z.Z. (14KJA320002), Jiangsu Specially Appointed Professorship to Z.Z. and Q.-Y.T., Natural Science Foundation of China (NSFC) Grants 81471314 and 81671090 to Z.Z., Natural Science Foundation of Jiangsu Province Grant SBK201502515 to Z.Z., Xuzhou Science and Technology Program Grants KC19036 to Z.Z. and KC16H0230 to Q.-Y.T., NSFC Grant 31671212 to Q.-Y.T.; Priority Academic Program Development of Jiangsu Higher Education Institutions and the Jiangsu Provincial Special Program of Medical Science Grant BL201402, Postgraduate Research & Practice Innovation Program of Jiangsu Province Grant KYCX21\_2708 to Q.Z., and College Students Innovation and Entrepreneurship Training Program Grants 201510313034Y to S.-H.G. and 201810313017Z to Y.W.

\*Q.Z., S.-H.G., Z.-S.S., Y.W., and S.-W.H. contributed equally to this work.

The authors declare no competing financial interests.

Correspondence should be addressed to Qiong-Yao Tang at qiongyaotang@hotmail.com or Zhe Zhang at Zhangzhe70@xzhmu.edu.cn.

<https://doi.org/10.1523/JNEUROSCI.2027-21.2022>

Copyright © 2022 the authors

## Introduction

Anxiety disorder, characterized by excessive fear or anxiety, is a type of mental health condition caused by a combination of genetic and environmental factors (Gottschalk and Domschke, 2017). Many efforts have been made to identify single genes that are associated with anxiety disorders, but there has been no clear conclusion until recently (Howe et al., 2016). Previous studies suggest that overexpression of the SK2 channel in basolateral amygdala (BLA) neurons reduces anxious behaviors (Mitra et al., 2009; Zhang et al., 2019). In addition to the SK2 channel, the involvement of the hyperpolarization-activated cyclic nucleotide-gated (HCN) channel, TMEM74, and ASIC1a channel in the regulation of anxiety-like behaviors has also been reported (Park et al., 2011; Pidoplichko et al., 2014; Shao et al., 2019).

Thus, the malfunction of ion channels may lead to anxiety disorders.

On the other hand, the amygdala has been identified as an integrative center in the regulation of anxiety responses (LeDoux, 2007; Mitra et al., 2009; Felix-Ortiz et al., 2013; Li et al., 2019; Salimando et al., 2020), especially the BLA and its associated neuronal circuits. The overactivation of the glutamatergic BLA inputs to the ventral hippocampus (vHPC) resulting in anxiety has been identified (Felix-Ortiz et al., 2013), but the molecular and cellular determinants in BLA–vHPC projections for anxiety disorders are still not well understood.

The Slack (sequence like a  $\text{Ca}^{2+}$ -activated  $\text{K}^+$  channel) channel is encoded by the *Kcnt1* gene (Yuan et al., 2003). As a member of the large-conductance  $\text{Ca}^{2+}$ - and voltage-activated  $\text{K}^+$  channel family (Mullen et al., 2018), the Slack channel is activated by intracellular sodium and chloride ions and possesses a relatively large single conductance (Yuan et al., 2003; Zhang et al., 2010). The Slack channel protein is abundantly expressed in the CNS of mammals, including the olfactory bulb, hippocampus, amygdala, frontal cortex, thalamus, and some other brain regions (Bhattacharjee et al., 2002; Brown et al., 2010; Lu et al., 2010; Cervantes et al., 2013; Rizzi et al., 2016). It plays critical roles in various physiological and pathophysiological processes such as spatial learning, nociceptive sensing, fragile X syndrome, and a wide spectrum of seizure disorders (Brown et al., 2010; Zhang et al., 2012; Bausch et al., 2015; Lu et al., 2015; Moller et al., 2015; Evely et al., 2017).

In the present study, we demonstrate that gain or loss of function of Slack channel mice exhibit anxiolytic and anxiogenic behaviors, respectively. Abnormal Slack channel function-induced glutamatergic BLA–vHPC neuronal excitability alterations contribute to anxiety-related behaviors. Our data reveal the role of the Slack channel in the regulation of anxiety, which may provide a potential molecular target for anxiolytic therapies.

## Materials and Methods

**Animals.** Four strains of mice were used in this study: C57BL/6J mice, *Slack KO* (Deltagen), *Kcnt1 Y777H* mutant (Nanjing Biomedical Research Institute of Nanjing University) and Slack conditional knockout (CKO; GemPharmatech) mice on a C57BL/6J background. The generation strategy is shown in Figures 1A, 2A, and 7A, respectively. To generate *Slack KO* mice, the exon7–exon11 of the *Kcnt1–201* (ENSMUST00000037580) were replaced by LacZ-NEO cassette. The *Y777H* mutation was introduced into exon 21 of the *Kcnt1–201* transcript to generate *Kcnt1 Y777H* mice. The target sequences to generate *Slack CKO* mice is exon2–exon32 of the *Kcnt1–201* transcript, which contains 3562 bp coding sequence. The genotype of pups was detected by PCR. Male mice aged 7–8 weeks were used in this study. All mice were housed four or five per cage under a 12 h light/dark cycle with food and water available *ad libitum*.

**Behavioral tests.** The Elevated Plus Maze (EPM) tests were performed as described previously (Hu et al., 2021). The Elevated Plus Maze consists of two open arms (30 cm × 5 cm) and two closed arms (30 cm × 5 cm) elevated 70 cm above the ground. A digital camera above the maze was used to record the traces of mice. Mice were placed at the center between the open and closed arms and allowed to explore freely for 300 s. The avoidance behavior was measured by time spent in open arms and the probability of open arm entry. Traveling traces were recorded by the ANY-maze system.

The open field (OF) test was conducted as described previously (Xia et al., 2020). Mice were placed in the center of a square chamber (40 cm × 40 cm) for 600 s following sterilization by 75% alcohol. The center zone is a 20 cm × 20 cm area in the center part of the chamber. The avoidance behavior was measured by time spent in the center zone and

the number of center zone entries. Traveling traces were recorded by the ANY-maze system.

For the Forced Swim Test (FST), mice were placed into a transparent Plexiglas cylinder (18 cm in diameter; 40 cm high) filled with 25°C tap water to a depth of 25 cm for 300 s. Depression-like behavior was measured by the duration of immobility in the last 240 s.

Before the sucrose preference test (SPT), mice were placed into individual cages with tap water or 1% sucrose available *ad libitum* in two bottles to adapt to the test. The adaption lasted for 24 h, and the two bottles were exchanged every 12 h to avoid position preference. The following 2 h or 24 h intake of tap water and 1% sucrose were weighted. Preference behavior was reflected by the percentage of sucrose intake.

For the tail-suspension test (TST), mice were suspended 30 cm above the floor with tails adhered to an apparatus. The test lasted for 300 s, and the immobility of each mouse during the last 240 s was recorded.

The fear conditioning test was conducted in conditioning chambers (catalog #ENV-414SA, Med Associates) as previously described (Dedic et al., 2018). On day 0, mice were subjected to a fear conditioning protocol with 2 conditioned stimulus–unconditioned stimulus (tone-shock) pairings (80 dB, 9 kHz, 20 s tone coterminated with 1.5 mA, 2 s electric foot shock) for delay conditioning. On day 1, mice were placed back into the original fear context lasting 180 s for contextual retrieval. On day 2, mice were placed into a novel environment with a 180 s tone (80 dB, 9 kHz) for cued retrieval. Contextual and cued fear learning was measured by freezing behavior exerted in associated retrieval.

For the light-dark box test, a dark box (12 cm × 12 cm) with a small opening was inserted in the center part of the light box (40 cm × 40 cm). Mice were placed inside the dark box and allowed to freely explore for 300 s. Latency to the light box and total time spent in the dark box was noted.

**Corticosterone treatment.** Corticosterone (CORT) treatment was conducted by allowing free access to either 0.1 mg/ml CORT (catalog #C805819, Macklin) dissolved in ethanol (1% ethanol final concentration) or vehicle (1% ethanol solution) instead of drinking water. This exposure lasted for 3 weeks (Peng et al., 2021).

**RNA extraction and qRT-PCR.** RNA extraction and qRT-PCR were performed as described previously (Pan et al., 2021). In brief, total RNA was extracted using RNAiso Plus protocol (catalog #9109, Takara) and reversely transcribed into cDNA using HiScript II Reverse Transcriptase (catalog # R223-1, Vazyme). qPCR was conducted with Light Cycler 480 II (Roche Diagnostics) using a TB Green reaction system (catalog #RR820, Takara). The quantification of *Kcnt1* standardized by *Gapdh* and the expression levels of the target gene was analyzed by the  $2^{-\Delta\Delta CT}$  method. The sequences of primers (Sangon Biotech): *Kcnt1*, CACCA TCACCAGGCTGCTCTTG (forward) and GTCGTCCTCGGTTA CCTTCATTGC (reverse); *Gapdh*, GGTGAAGGTCGGTGTGAACG (forward) and CTCGCTCCTGGAAGATGGTG (reverse).

**Western blot.** Western blot analysis was performed as in our previous studies. Briefly, proteins (40  $\mu\text{g}$ /sample) were extracted, transferred onto PVDF membranes, and incubated at 4°C overnight with the primary SLACK antibody (1:1000; NeuroMab, clone N3/26), Flag antibody (1:1000; catalog #ab1162, Abcam) and Beta ACTIN antibody (1:2000; 66009-1-Ig, Proteintech). The membranes were then washed and incubated with the secondary antibody (1:2000; catalog #A0216/A0208, Beyotime) with HRP label. The bands were visualized by nitro blue tetrazolium/5-bromo-4-chloro-3-indolyl-phosphate assay kit (catalog #72091, Sigma-Aldrich). Beta ACTIN was used as a reference protein.

**Adenovirus-associated virus.** The following adenovirus-associated viruses (AAVs) were purchased from Tailor, Brain VTA, and OBIO Technology: AAV-hSyn-r*Kcnt1*-3flag-sv40-ployA (2/9, 2.28E+12 vg/ml), AAV-hSyn-eGFP-WPRE-SV40pA (2/9, 2.01E+12 vg/ml), AAV-CaMKII-Cre-WPRE-pA (2/9, 5.63E+12 vg/ml), AAV-hSyn-DIO-r*Kcnt1*-3flag-SV40pA (2/9, 5.13E+12 vg/ml), AAV-EF1 $\alpha$ -DIO-mCherry-WPRE-hGH pA (2/9, 5.00E+12 vg/ml), AAV-CaMKII-Cre-mCherry-WPRE-pA (2/9, 5.00E+12 vg/ml), AAV-CaMKII $\alpha$ -2A-Cre (2/Retro, 2.16E+12 vg/ml), AAV-CaMKII-mCherry-WPRE-pA (2/9, 5.00E+12 vg/ml).

**Stereotaxic surgery.** Mice weighing 23–25 g were anesthetized with 1% pentobarbital (40 mg/kg, i.p.) and secured on a small-animal

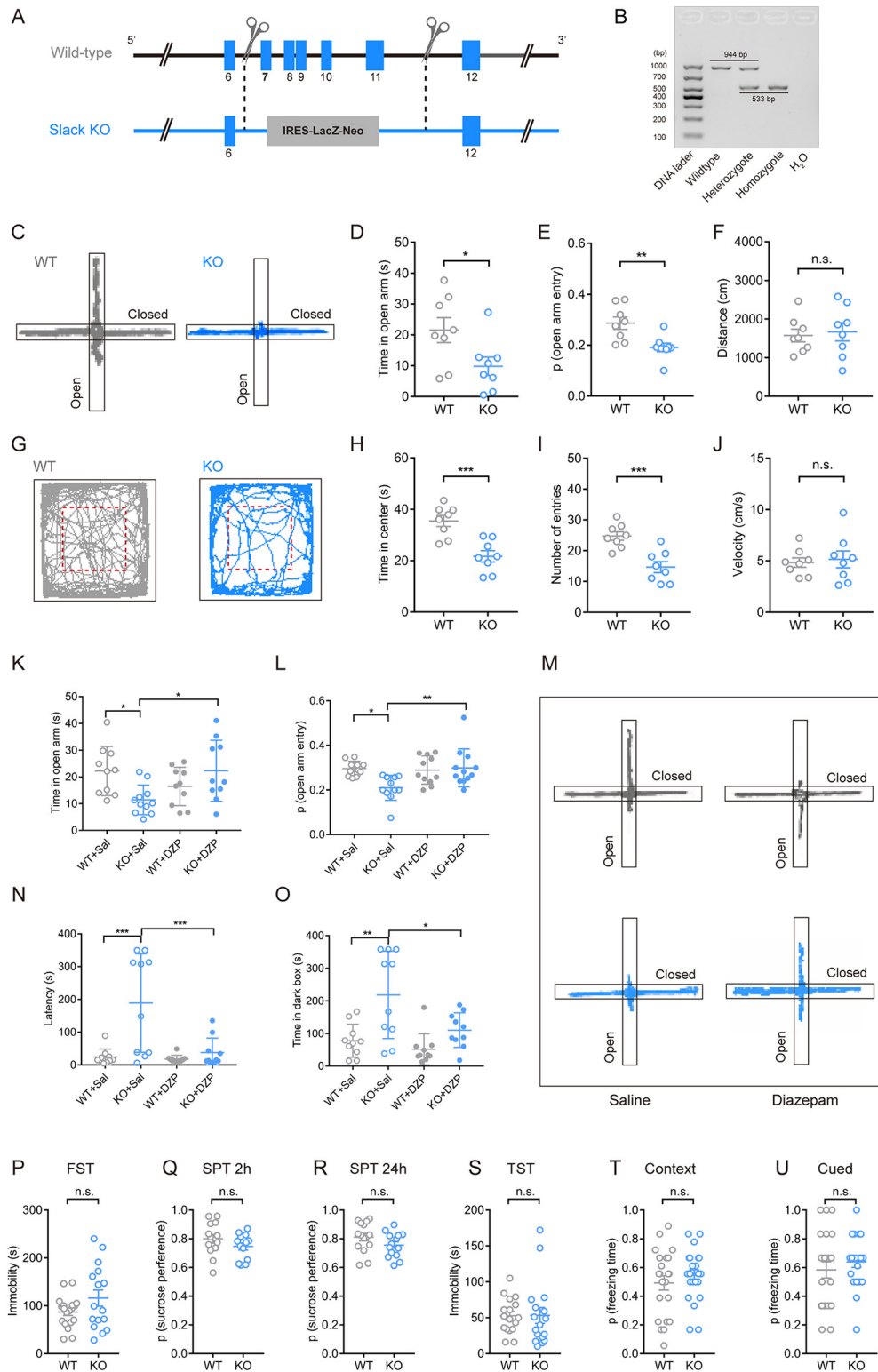


**Figure 1.** *Slack* KO mice exhibit enhanced avoidance behaviors but with normal depression-related behaviors and normal fear memory. **A**, Schematic diagram of Slack knock-out strategy. **B**, PCR verification of targeted axons deletion in *Slack* KO mice. **C–F**, *Slack* KO mice display enhanced avoidance behaviors in EPM test (**C–F**) and OF test (**G–J**). Representative trajectories of WT mice (left) and Slack KO mice (right) in EPM exploration (**C**). Time spent in the anxiogenic open arms (**D**). Probability of open-arm entry (**E**). Total distance traveled in EPM (**F**). Two-tailed unpaired *t* test,  $n = 8$ ,  $*p < 0.05$  (**D**);  $n = 8$ ,  $**p < 0.01$  (**E**);  $n = 8$ , n.s. (**F**). Representative trajectories of OF exploration (**G**). Time spent in the OF center (**H**). Number of entries into the OF center (**I**). Velocity traveled in OF (**J**). Two-tail unpaired *t* test,  $n = 8$ ,  $***p < 0.001$  (**H**);  $n = 8$ ,  $***p < 0.001$  (**I**);  $n = 8$ , n.s. (**J**). Intraperitoneal injection of DZP (1 mg/kg) reduces avoidance behaviors of Slack KO mice in the EPM test (**K–M**) and light-dark box test (**M**, **O**). Time spent in the anxiogenic open arms (**K**). Probability of open-arm entry (**L**). Representative trajectories of EPM exploration (**M**). One-way ANOVA in **K**, **L**;  $n = 10–12$ ,  $*p < 0.05$ ,  $**p < 0.01$ . **N**, Latency to the first entry to the light box. **O**, Time spent in the dark box. One-way ANOVA (**N**, **O**),  $n = 10–12$ ,  $*p < 0.01$ ,  $**p < 0.05$ ,  $***p < 0.001$ . **P–S**, The *Slack* KO mice did not show significantly different depressive behavior from WT mice in FST (**P**), SPT 2 h and 24 h (**Q**, **R**), and TST (**S**). **T**, **U**, The *Slack* channel knock-out mice show normal contextual fear learning (**T**) or cued fear learning (**U**). Two-tail unpaired *t* test,  $n = 13–22$  (**P–U**). Data are presented as mean  $\pm$  SEM. The details of the data are provided in Extended Data Figure 1-1. n.s., Not significant.

stereotaxic frame (RWD). After disinfection and exposure of cranium, viruses of 150–200 nl were injected bilaterally into the BLA [anteroposterior,  $-1$  mm; mediolateral (ML),  $\pm 3.22$  mm; dorsoventral (DV),  $5.2$  mm], vHPC (anteroposterior,  $-3.0$  mm; ML,  $\pm 3.1$  mm; DV,  $4.0$  mm) and dorsomedial prefrontal cortex (dmPFC; anteroposterior,  $1.94$  mm; ML,  $\pm 0.35$  mm; DV,  $2.3$  mm) at a rate of  $0.1$  nl/min by a Hamilton syringe needle (33 gauge) coupled to a pump. Injectors were slowly retracted after a 7–8 min diffusion period. The mice were cared to recover for 3–4 weeks before experiments.

**RNA*scope* in situ hybridization.** Mice (C57/BL6, 8 weeks) were anesthetized with 1% pentobarbital (40 mg/kg, i.p.), and mice brains were isolated after perfusion with 0.9% saline and 4% freshly prepared PFA. After overnight PFA treatment and 48 h of dehydration by sucrose solution, sections of  $20 \mu\text{m}$  thick were prepared by a freezing microtome (VT1000S, Leica Microsystems). For examination of KCNT1, VGLUT1, and VGAT expression in BLA, slices were processed for fluorescent *in situ* hybridization by RNAscope Multiplex Fluorescent Reagent Kit V2 (catalog #323100, ACD) according to manufacturer guidelines. The probes used were *V-gat* (RNAscope Probe-Mm-Slc32a1, 319191-C1, ACD), *Kcnt1* (RNAscope Probe-Mm-probes-Kcnt1, 492491-C2, ACD), and *V-glut1* (RNAscope Probe-Mm-Slc17a7, 416631-C3, ACD). DAPI staining was performed to label the nuclei of cells. Finally, the prepared slices were imaged by a confocal microscope (LSM 880, Zeiss).

**Slice preparation.** Mice (8–12 weeks) were anesthetized with sevoflurane. Following quick removal of brains,  $300\text{-}\mu\text{m}$ -thick slices were cut with a vibratome (Leica) in ice-cold sucrose-based cutting solution, which contained the following (in mM): 2.5 KCl, 85 NaCl, 1.25  $\text{NaH}_2\text{PO}_4$ , 4  $\text{MgCl}_2$ , 0.5  $\text{CaCl}_2$ , 24  $\text{NaHCO}_3$ , 25 Glucose, and 75 sucrose, pH 7, and an osmolarity of 310–320 mOsm. Slices were incubated in the cutting solution for  $\sim 15$  min at  $37^\circ\text{C}$ . Finally, the slices were then transferred into a recording chamber, consistently perfused with oxygenated artificial cerebrospinal fluid (ACSF) at a rate of 4 ml/min before electrophysiological recordings at room temperature. The ACSF solution contained the following (in mM): 126 NaCl, 2.5 KCl, 1.2  $\text{NaH}_2\text{PO}_4$ , 1.2  $\text{MgSO}_4$ , 2.4  $\text{CaCl}_2$ , 26  $\text{NaHCO}_3$ , and 10 Glucose, pH of 7, and an osmolarity of 300–320 mOsm. All external solutions were oxygenated with 95%  $\text{O}_2$  and 5%  $\text{CO}_2$ .

**Whole-cell recording in brain slice.** Neurons were visualized by an upright IX 51 microscope (Olympus) with a  $40\times$  water immersion objective. Patch pipettes (6–10 M $\Omega$ ) of borosilicate glass 9 (Sutter) were made by a P-97 horizontal micropipette puller (Sutter). The pipette solution contained the following (in mM): 130 potassium gluconate, 5 KCl, 4  $\text{Na}_2\text{ATP}$ , 0.5  $\text{NaGTP}$ , 20 HEPES, 0.5 EGTA, pH 7.4, with KOH 7.4, 310–320 mOsm. Data were acquired with pClamp 10.2 software (Molecular Devices) using a MultiClamp 700B patch-clamp amplifier and a Digidata 1440A (Molecular Devices). The current was pass filtered on-line at 1 kHz, and the stimulation from  $-30$  pA to  $150$  pA was enhanced by  $10$  pA per sweep under the current clamp.

**Statistical analysis.** Statistical analyses were conducted with Prism 7.0 software (GraphPad) with the appropriate method illustrated in the figure legends. All data were analyzed with a two-tailed test and represented as mean  $\pm$  SEM. Unpaired *t* test was used for two-group comparisons. One-way ANOVA followed by a Bonferroni post test was used for three or four group comparisons. Two-way ANOVA followed by a

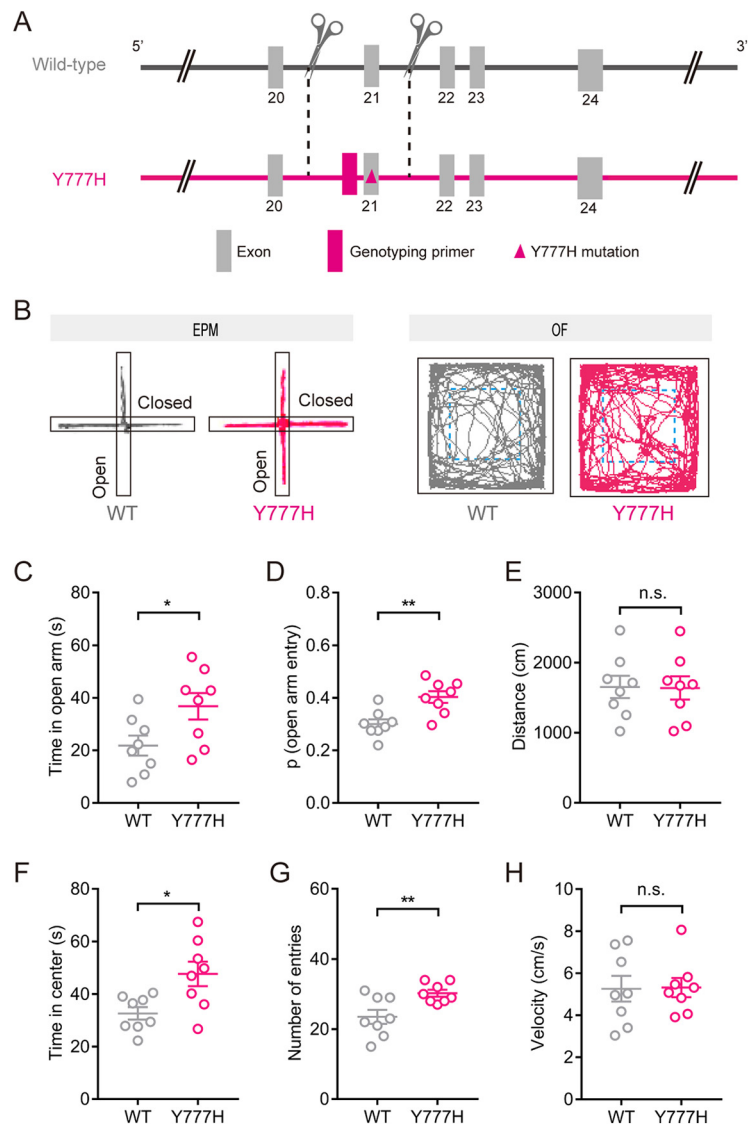


**Figure 2.** The *Slack*-Y777H gain-of-function mutant mice exhibit anxiolytic behaviors. **A**, Scheme of generating the *Slack* Y777H mutant strategy. **B–H**, *Slack* Y777H gain-of-function mutant mice exhibit anxiolytic behaviors in the EPM test (**B–E**) and OF test (**B, F–H**). Representative trajectories of EPM and OF exploration (**B**). Time spent in the open arms (**C**). Probability of open-arm entry (**D**). Total distance traveled in EPM (**E**). Two-tail unpaired *t* test,  $n = 8$ ,  $*p < 0.05$  (**C**);  $n = 8$ ,  $**p < 0.01$  (**D**);  $n = 8$ , n.s. (**E**). Time spent in the OF center (**F**). Number of entries into the center (**G**). Moving velocity (**H**). Two-tail unpaired *t* test,  $n = 8$ ,  $*p < 0.05$  (**F**);  $n = 8$ ,  $**p < 0.01$  (**G**);  $n = 8$ , n.s. (**H**). Data are presented as mean  $\pm$  SEM. The details of the data are provided in Extended Data Figure 1–1. n.s., Not significant.

Bonferroni post test was used in action potential (AP) analysis. Data are considered to be statistically significant if  $p < 0.05$ .

## Results

### *Slack* KO mice exhibit enhanced avoidance behaviors but with normal depression-related behaviors and normal fear memory

To test the role of the Slack channel in anxiety, we first examined the behaviors of *Slack* knock-out (KO) mice in the EPM and OF test, which reflect the approach and/or avoidance behaviors of mice (Carola et al., 2002). The *Slack* (*Kcnt1*) KO mice were generated by replacing the chromosome fragment including 7–11 *Kcnt1* exons, which encode the pore domain of the Slack channel, with the inserted LacZ gene that encodes the enzyme  $\beta$ -galactosidase (Fig. 1A). The Slack knock-out mice were verified by PCR (Fig. 1B). Compared with the wild-type (WT) mice, *Slack*

KO mice spent less time and made significantly fewer entries into the open arms of the EPM (Fig. 1C–E; unpaired *t* test; *D*,  $t_{(14)} = 2.343$ ,  $p = 0.0344$ ; *E*,  $t_{(14)} = 3.212$ ,  $p = 0.0063$ ). The details of the data in the experiment are shown in Extended Data Figure 1–1. Moreover, the alteration of the exploratory behaviors of the mice cannot be attributed to the motor deficit because the total distance of both groups of mice traveled is not significantly different (Fig. 1F; unpaired *t* test;  $t_{(14)} = 0.3258$ ,  $p = 0.7494$ ). Similarly, in the OF test, the Slack KO mice spent less time and made fewer entries into the center of the open field than the WT mice without altering the averaged traveling velocity (Fig. 1G–J; unpaired *t* test; *H*,  $t_{(14)} = 4.439$ ,  $p = 0.0006$ ; *I*,  $t_{(14)} = 4.485$ ,  $p = 0.0005$ ; *J*,  $t_{(14)} = 0.3334$ ,  $p = 0.7438$ ). Next, to test whether the altered exploratory behaviors can be attributed to anxiety, we treated the Slack KO mice with anxiolytic drug diazepam and observed their exploratory behaviors in the EPM and light-dark box tests. The avoidance behaviors of the Slack KO mice were significantly attenuated in the EPM test performed 30 min after intraperitoneal injection of diazepam (DZP, 1 mg/kg) but were not attenuated in the normal saline (Sal) group (Fig. 1K–M; one-way ANOVA with Bonferroni post tests; *K*,  $F_{(3,37)} = 3.941$ ,  $p = 0.0155$ ;  $p = 0.0383$  WT + Sal vs KO + Sal;  $p = 0.0361$  KO + Sal vs KO + DZP; *L*,  $F_{(3,41)} = 5.083$ ,  $p = 0.0044$ ;  $p = 0.0159$  WT + Sal vs KO + Sal;  $p = 0.0093$  KO + Sal vs KO + DZP) Consistent with the results in the EPM test, the Slack KO mice in the diazepam administration group spent a significantly shorter time entering the light box for the first time and less time in the dark box than the KO mice in the saline group. After diazepam treatment, the latency to the first entry and time spent in the dark zone of the KO mice were not significantly different from those of the wild-type littermates in the control group (Fig. 1M,O; one-way ANOVA with Bonferroni post tests; *N*,  $F_{(3,36)} = 10.54$ ,  $p < 0.0001$ ;  $p = 0.0003$  WT + Sal vs KO + Sal;  $p = 0.0009$  KO + Sal vs KO + DZP; *O*,  $F_{(3,36)} = 8.394$ ,  $p = 0.0002$ ;  $p = 0.0022$  WT + Sal vs KO + Sal;  $p = 0.028$  KO + Sal vs KO + DZP). All these data indicate that the altered exploratory behaviors of the Slack KO mice should be explained as anxiety. As anxiety could be one of the key features of major depressive disorder (Huang et al., 2019), we continuously examined whether the Slack KO mice exhibited depression behaviors using FST (Fig. 1P), SPT (Fig. 1Q–R, 2 h and 24 h, respectively), and TST (Fig. 1S). Interestingly, the Slack KO mice did not show a statistically significant difference from WT mice in these tests (unpaired *t* test (*P*–*R*); *N*,  $t_{(33)} = 1.687$ ,  $p = 0.1009$ ; *O*,  $t_{(25)} = 1.373$ ,  $p = 0.1820$ ; *P*,  $t_{(27)} = 1.581$ ,  $p = 0.1256$ ; unpaired *t* test with Welch's correction (*S*),  $t_{(24,56)} = 0.04,614$ ,  $p = 0.9636$ ), indicating the important role of the Slack channel in the regulation of anxiety rather than depression.

Because fear and anxiety share common neuronal circuit mechanisms, we try to distinguish whether the anxious behaviors of the Slack channel are related to fear memory (Kjelstrup et al., 2002; Tovote et al., 2015). Thus, we performed a Pavlovian fear conditioning test by exposing the WT mice or Slack KO mice to foot shocks that paired with a tone. Then the cued fear response to tone was examined to test the role of the Slack channel in fear memory. Surprisingly, WT mice and Slack KO mice showed comparable freezing responses in contextual and cued retrieval trails (Fig. 1T–U; unpaired *t* test; *T*,  $t_{(42)} = 0.8448$ ,  $p = 0.4030$ ; *U*,  $t_{(42)} = 0.8153$ ,  $p = 0.4195$ ). Together, these data indicate that the Slack KO mice manifest anxiety-like behaviors but exhibit neither depression-like behaviors nor fear memory deficits.

### The Slack-Y777H gain-of-function mutant mice exhibit anxiolytic behaviors

To further investigate the role of the Slack channel in anxiety disorders, we tested the exploration behaviors of Slack-Y777H mutant mice (Fig. 2A). Y777H mutant is a gain-of-function Slack channel characterized in our previous study, which shows the most elevated sensitivity to sodium and the highest maximal  $P_o$  among the 12 examined mutations associated with epilepsy (Tang et al., 2016). In the EPM test, Y777H mice tended to spend more time and make more entries into the open arms than the WT mice (Fig. 2B–D; unpaired *t* test; *C*,  $t_{(14)} = 2.371$ ,  $p = 0.0326$ ; *D*,  $t_{(14)} = 3.61$ ,  $p = 0.0028$ ). In the OF test, Y777H mice spent more time and made more entries into the center of the OF than the WT mice (Fig. 2B,F–G; unpaired *t* test; *F*,  $t_{(14)} = 2.873$ ,  $p = 0.0123$ ; *G*,  $t_{(14)} = 3.011$ ,  $p = 0.0094$ ). In addition, no significant difference in moving distance and velocity was found in both tests, reflecting that those heightened exploratory behaviors were not caused by motor deficits (Fig. 2E,H; unpaired *t* test; *E*,  $t_{(14)} = 0.06,389$ ,  $p = 0.9500$ ; *H*,  $t_{(14)} = 0.07,223$ ,  $p = 0.9434$ ). EPM and OF results demonstrate that the Y777H mice exhibit anxiolytic behaviors.

### The Slack channel regulates anxiety-like behaviors in basolateral amygdala neurons

To investigate the relationship between the Slack channel and pathologic anxiety, we first detected the Slack channel mRNA expression level in anxiety-related brain regions in chronic CORT anxiety model mice (Fig. 3A). After 3 weeks of CORT exposure, the model mice, with significantly decreased body weight (Fig. 3B; unpaired *t* test; day 0,  $t_{(12)} = 0.259$ ,  $p = 0.8000$ ; day 21,  $t_{(12)} = 10.03$ ,  $p < 0.0001$ ), exhibited enhanced avoidance behaviors in the EPM (Fig. 3F–H; unpaired *t* test; *G*,  $t_{(11)} = 2.618$ ,  $p = 0.0239$ ; *H*,  $t_{(11)} = 2.343$ ,  $p = 0.0390$ ) and OF test (Fig. 3J–L; unpaired *t* test; *K*,  $t_{(12)} = 3.381$ ,  $p = 0.0055$ ; *L*,  $t_{(12)} = 2.545$ ,  $p = 0.0257$ ). Meanwhile, no significantly different locomotor activity (basic movements and distance moved in the maze) was found between the CORT model and control mice (Fig. 3I,M; unpaired *t* test; *I*,  $t_{(12)} = 0.7721$ ,  $p = 0.4550$ ; *M*,  $t_{(12)} = 0.05,722$ ,  $p = 0.9553$ ). Subsequently, qPCR was used to detect the *Kcnt1* mRNA expression in anxiety-related brain regions of the CORT model mice. The *Kcnt1* mRNA level was downregulated in the BLA but was not altered in other brain regions in the model mice [Fig. 3C,D; unpaired *t* test in C; BLA, Welch's correction,  $t_{(2,293)} = 4.531$ ,  $p = 0.0349$ ; central nucleus of the amygdala (CeA),  $t_{(4)} = 0.669$ ,  $p = 0.5401$ ; medial prefrontal cortex (mPFC),  $t_{(4)} = 0.1398$ ,  $p = 0.9855$ ; hippocampus (Hip),  $t_{(4)} = 0.8917$ ,  $p = 0.4229$ ; CeA,  $t_{(4)} = 0.669$ ,  $p = 0.5401$ ; cerebellum (Cb),  $t_{(4)} = 0.2512$ ,  $p = 0.8141$ ; lateral habenular nucleus (LHb), Welch's correction,  $t_{(2,027)} = 0.04,248$ ,  $p = 0.9699$ ; bed nucleus of the stria terminalis (BNST),  $t_{(4)} = 0.6607$ ,  $p = 0.5449$ ; periaqueductal gray (PAG),  $t_{(4)} = 0.08,366$ ,  $p = 0.9373$ ]. Also, we performed Western blot and found that consistent with the alteration of mRNA level, the Slack protein level was decreased in the BLA of CORT model mice (Fig. 3E; unpaired *t* test;  $t_{(6)} = 5.444$ ,  $p = 0.0016$ ). This result suggests the Slack channel may play its role in regulating anxiety-like behaviors in the BLA. To test this hypothesis, we expressed the *Kcnt1* gene in the BLA of Slack KO mice by injecting the AAV-hSyn-*Kcnt1*-3flag virus into the BLA of the Slack channel KO mice. Meanwhile, the AAV-hSyn-eGFP-3flag virus was injected into the BLA of KO mice in the control group (Fig. 4A,B, middle). The *Kcnt1* gene expression in the BLA was validated by Western Blot using

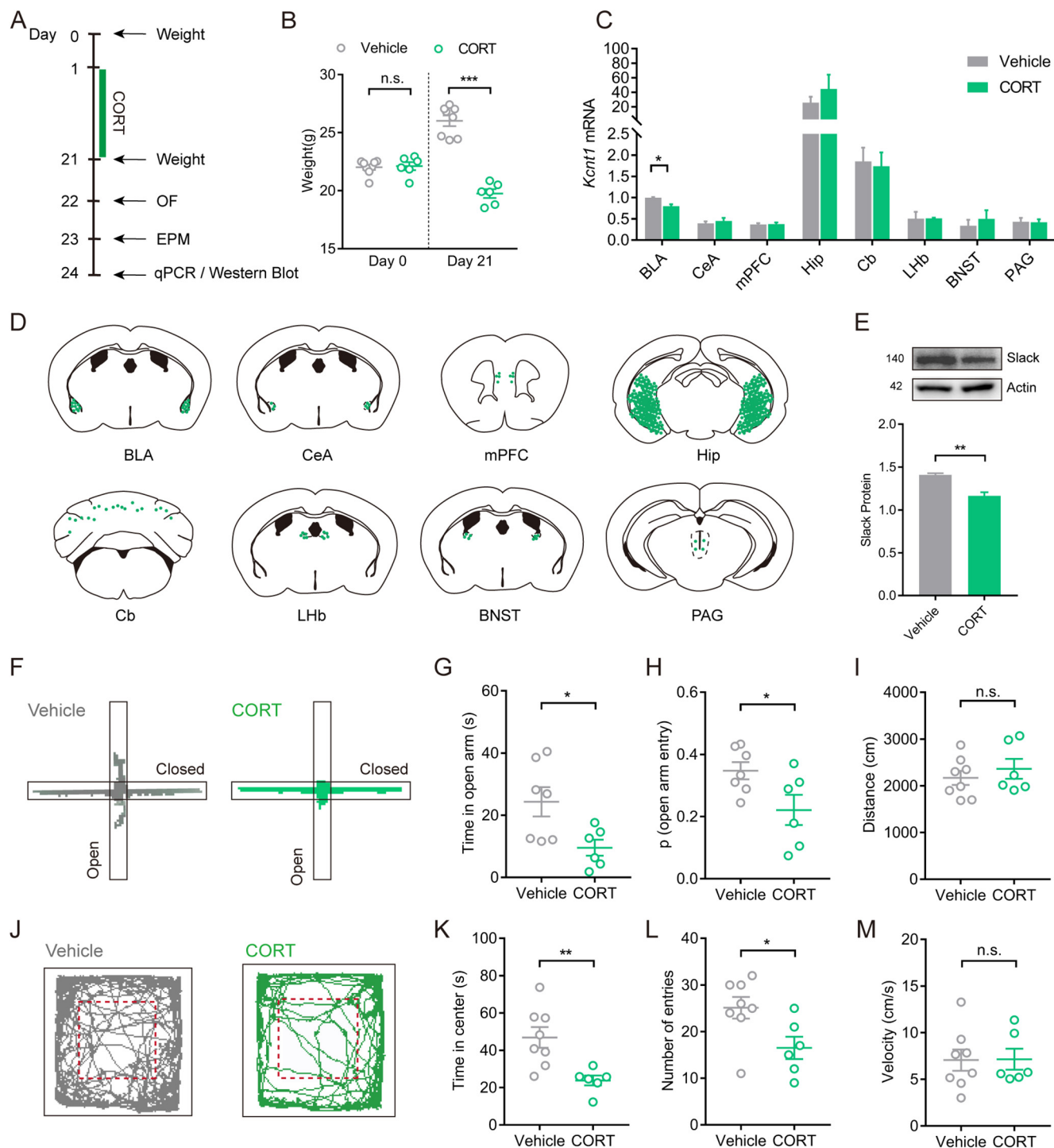


**Figure 3.** Chronic CORT treatment decreases Slack expression in the BLA. **A**, Timeline of measuring body weight, chronic CORT exposure, and anxiety-like behavioral test. **B**, Body weight of mice before (day 0) and after (day 21) chronic CORT exposure. **C**, The *Kcnt1* mRNA expression levels in different brain regions of vehicle-treated mice and CORT mice, normalized to the BLA *Kcnt1* mRNA expression level in vehicle-treated mice. The two-tailed unpaired *t* test,  $n = 8$  for Vehicle and  $n = 6$  for CORT, n.s.,  $***p < 0.001$  (**B**);  $n = 3$ ,  $*p < 0.05$  (**C**). **D**, Schematic diagram of *Kcnt1* mRNA expression in anxiety-related brain regions. The number of green plots presents the expression level of *Kcnt1* mRNA in the vehicle group. **E**, The Slack protein expression in the BLA of vehicle-treated mice and CORT mice; two-tailed unpaired *t* test,  $n = 4$ ,  $**p < 0.01$ . **F–M**, Chronic CORT treatment increased avoidance behaviors of mice in the EPM test (**F–I**) and OF test (**J–M**). Representative trajectories of EPM exploration (**F**). Time spent in the open arms (**G**). Probability of open-arm entry (**H**). Total distance traveled in EPM (**I**). Representative traces trajectories of OF exploration (**J**). Time spent in the center (**K**). Number of entries into the center (**L**). Moving velocity (**M**); two-tailed unpaired *t* test,  $n = 7–8$  for Vehicle and  $n = 6$  for CORT mice,  $*p < 0.05$  (**G**),  $*p < 0.05$  (**H**), n.s. (**I**),  $**p < 0.01$  (**K**),  $*p < 0.05$  (**L**), n.s. (**M**). Data are presented as mean  $\pm$  SEM. The details of the data are provided in Extended Data Figure 1–1. n.s., Not significant.

extracted protein from BLA of mice (Fig. 4B, left), whereas the eGFP fluorescence was detected in the BLA of the control mice (Fig. 4B, right). Interestingly, the enhanced avoidance behaviors of the Slack channel knock-out mice were

abolished by the *Kcnt1* gene expression in BLA neurons (Fig. 4C–E; unpaired *t* test in **D** and **E**; **D**,  $t_{(14)} = 2.822$ ,  $p = 0.0136$ ; **E**,  $t_{(14)} = 4.286$ ,  $p = 0.0008$ ). Thus, the Slack channel expression in the BLA neurons plays an anxiolytic role.

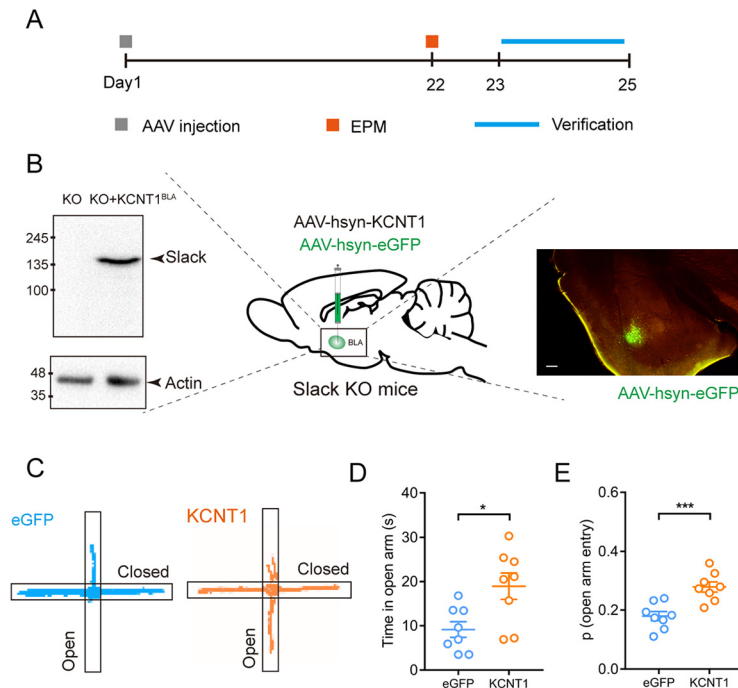


**Figure 4.** Compensatory expression of Slack channel in BLA neurons rescues the enhanced avoidance behaviors of the global *Slack* knock-out mice. **A**, Timeline of AAV injection, EPM test, scarification, and verification. **B**, Schematic diagram of a compensatory expression of the Slack channel by injection adeno-associated viral that carried the Flag-tagged *Kcnt1* gene in the BLA of *Slack* KO mice (middle), Western blot bands (left) and fluorescent images confirmed the successful expression of the Slack channel in the BLA (right). Scale bar, 200  $\mu$ m. **C**, Representative trajectories of EPM exploration. **D**, **E**, The Slack channel expression in BLA neurons decreased avoidance behaviors of *Slack* KO mice in the EPM test, shown as time spent in open arms (**D**) and probability of open-arm entry (**E**). Two-tailed unpaired *t* test,  $n = 8$ ,  $*p < 0.05$  (**D**);  $n = 8$ ,  $***p < 0.001$  (**E**). Data are presented as mean  $\pm$  SEM. The details of the data are provided in Extended Data Figure 1-1.

### The Slack channel regulates the glutamatergic neuronal excitability in the basolateral amygdala

To further distinguish the neuronal type in which the Slack channel plays its role in the BLA, we performed *in situ* hybridization using the RNAscope method to detect the neuronal distribution of the Slack channel mRNA. Consistent with previous studies (Tye et al., 2011), the BLA is composed of  $\sim 90\%$  glutamatergic (VGLU1-positive) neurons and 10% GABAergic (VGAT-positive) neurons (Fig. 5A). We further found that the *Kcnt1* mRNA expressed in 96.20% BLA glutamatergic neurons and 56.89% GABAergic neurons (Fig. 5A–C). Thus, Slack channels are predominantly expressed in BLA glutamatergic neurons. We subsequently performed the whole-cell current-clamp recording to investigate whether the Slack channel alters the activity of BLA glutamatergic neurons. Three weeks before recordings, AAV-CaMKII-Cre-mCherry was injected into the BLA of mice to label glutamatergic neurons (Fig. 5E). The typical AP (action potential) traces recorded from BLA glutamatergic neurons with red fluorescence signal from WT mice, *Slack* KO mice, and *Slack* Y777H mice are shown in Figure 5D. The BLA glutamatergic neurons of the *Slack* KO mice generated twofold more numbers of action potentials than the neurons of the WT littermates in response to the same depolarization current from 30 to 150 pA. In contrast, the BLA glutamatergic neurons of the Y777H mutant mice generated significantly fewer APs than the neurons in WT littermates in response to a given depolarization current (Fig. 5F; two-way ANOVA with Bonferroni's multiple comparisons test;  $F_{(2,760)} = 200$ ,  $p < 0.0001$ ;  $-30$  to  $-10$  pA:  $p > 0.9999$  WT vs KO,  $p > 0.9999$  WT vs Y777H;  $0$  pA:  $p > 0.9999$  WT vs KO,  $p =$

$0.9067$  WT vs Y777H;  $10$  pA:  $p = 0.9786$  WT vs KO,  $p = 0.4925$  WT vs Y777H;  $20$  pA:  $p = 0.0704$  WT vs KO,  $p = 0.3849$  WT vs Y777H;  $30$  pA:  $p = 0.048$  WT vs KO,  $p = 0.1830$  WT vs Y777H;  $40$  pA:  $p = 0.0006$  WT vs KO,  $p = 0.0794$  WT vs Y777H;  $50$  pA:  $p = 0.0004$  WT vs KO,  $p = 0.0665$  WT vs Y777H;  $60$  to  $150$  pA:  $p < 0.05$  WT vs KO,  $p < 0.05$  WT vs Y777H). Consistent with the results of firing rates, the averaged resting potential (RP) of BLA excitatory neurons of *Slack* KO mice was 4.1 mV higher than the RPs of neurons of the WT littermates. In contrast, the averaged resting potential of BLA glutamatergic neurons of Y777H mutant mice was 5.4 mV lower than that in WT mice (Fig. 5G; one-way ANOVA with Bonferroni's multiple comparisons test;  $F_{(2,38)} = 16.59$ ,  $p < 0.0001$ ;  $p = 0.0428$  WT vs KO,  $p = 0.0013$  WT vs Y777H). Because the Slack channel was previously reported to increase the amplitude of the slow afterhyperpolarization (sAHP; Lu et al., 2010; Cervantes et al., 2013); we also analyzed the AHP amplitude in BLA glutamatergic neurons. However, we failed to observe the sAHP in glutamatergic neurons in any phenotype mice. Also, no significant alteration of AHP amplitudes either in *Slack* KO mice or in Y777H mice was observed (Fig. 5H; one-way ANOVA with Bonferroni's multiple comparisons test;  $F_{(2,38)} = 1.221$ ,  $p = 0.3063$ ).

### The Slack channel regulates anxiety-like behaviors in the glutamatergic neurons of the basolateral amygdala

To address whether the Slack channel expression in BLA glutamatergic neurons can reverse the anxiety-like behaviors of *Slack* KO mice, the compensatory Slack channel expression in glutamatergic neurons was conducted by injection of AAV-CaMKII-Cre/AAV-DIO-*Kcnt1*-3flag mixture into the BLA of the *Slack* KO mice. We named the mice *Slack* KO<sup>BL-G-Kcnt1</sup> mice. The control *Slack* KO mice were injected with an AAV-CaMKII-Cre/AAV-DIO-mCherry mixture so that the expression of mcherry in glutamatergic neurons can be examined by their fluorescence. The control mice were named *Slack* KO<sup>BL-G-mcherry</sup> mice (Fig. 6A,B). After the validation of compensatory expression of the Slack channel (Fig. 6C), we tested the avoidance behaviors of these mice. Compared with *Slack* KO<sup>BL-G-mcherry</sup> mice, *Slack* KO<sup>BL-G-Kcnt1</sup> mice spent more time in the open arms and showed more entries into the open arms in the EPM test. Similarly, *Slack* KO<sup>BL-G-Kcnt1</sup> mice spent more time in the center and showed more entries into the center in the OF test, indicating the reduced avoidance behaviors. Moving distance and velocity in both groups of mice were not significantly different in the EPM and OF tests (Fig. 6D–K; unpaired *t* test in E–G, I–K); E,  $t_{(12)} = 2.565$ ,  $p = 0.0248$ ; F,  $t_{(12)} = 2.484$ ,  $p = 0.0287$ ; G,  $t_{(12)} = 1.731$ ,  $p = 0.1091$ ; I,  $t_{(12)} = 2.556$ ,  $p = 0.0252$ ; J,  $t_{(12)} = 2.548$ ,  $p = 0.0256$ ; K,  $t_{(12)} = 1.543$ ,  $p = 0.1488$ ). Similarly, no significant difference in depression and fear memory-related behaviors tests was observed between the two groups of mice (Fig. 6L–Q; unpaired *t* test; L,  $t_{(12)} = 0.4195$ ,  $p = 0.6822$ ; M,  $t_{(12)} = 0.5869$ ,  $p = 0.5682$ ; N,  $t_{(12)} = 0.19$ ,  $p = 0.8525$ ; O,  $t_{(12)} = 0.3603$ ,  $p = 0.7249$ ; P,  $t_{(12)} = 0.6819$ ,  $p = 0.5083$ ; Q,  $t_{(12)} = 0.06394$ ,  $p = 0.9501$ ). As a consequence of the Slack channel expression, the excitability of

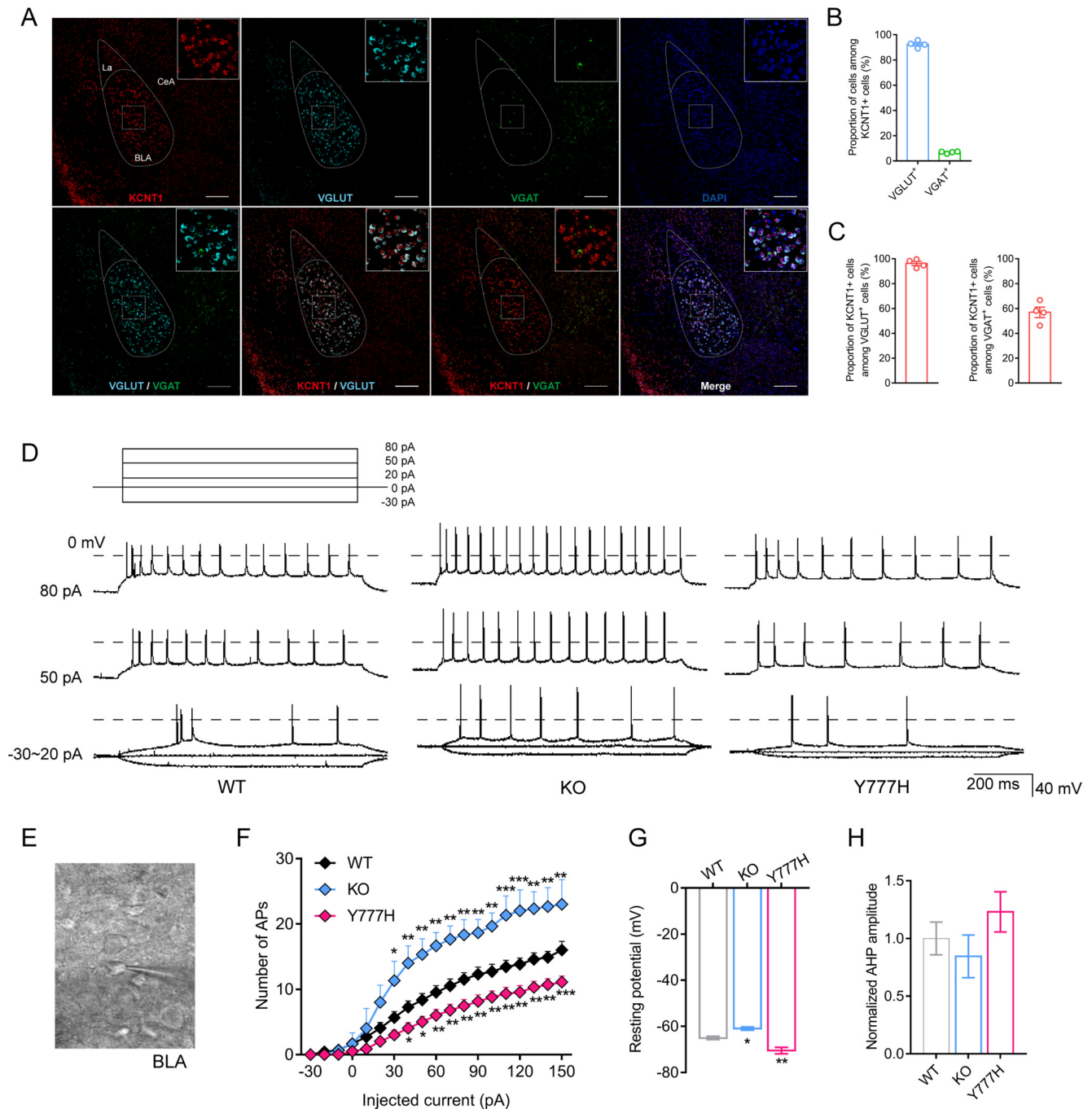


**Figure 5.** The Slack channel expresses in VGLUT-positive glutamatergic neurons in the basolateral amygdala and alters neural activities. **A**, Fluorescent images of *in situ* hybridization by RNA scope showing the distribution of *Kcnt1* (red), VGLUT (cyan), VGAT mRNA (green), and DAPI (blue) in the BLA. Scale bar, 200  $\mu\text{m}$ . **B**, Percentage of *Kcnt1* mRNA-positive neurons that express VGLUT and VGAT. **C**, Percentage of VGLUT-positive (left) and VGAT-positive (right) neurons that express *KCNT1* mRNA. **D**, Representative traces show the effect of injected current (–30 to 80 pA) induced action potentials in BLA CaMKII<sup>+</sup> neurons from WT mice (left), *Slack KO* mice (middle), and *Slack gain-of-function mutant (Y777H)* mice (right). **E**, Sample patch of brain slice in mice with CaMKII<sup>+</sup> neurons marked by mCherry fluorescence 21 d after injection of AAV-CaMKII-Cre-mCherry in the BLA. **F**, Numbers of APs induced by step current injection (–30 to 150 pA) in the CaMKII<sup>+</sup> neurons of the WT, *Slack KO*, and *Y777H* mutant mice. Data were analyzed by two-way ANOVA; 18 cells for WT, 9 cells for KO, and 16 cells for *Y777H* from three to five mice in each genotype; \* $p < 0.05$ , \*\* $p < 0.01$ , \*\*\* $p < 0.001$ . **G**, Average resting potentials in CaMKII<sup>+</sup> BLA neurons of WT, *Slack KO*, and *Y777H* mutant mice. Data analyzed by one-way ANOVA, 16 cells for WT, 9 cells for KO, and 16 cells for *Y777H*, from three to five mice in each group, \* $p < 0.05$ . **H**, Average AHP in these neurons from WT, *Slack KO*, and *Y777H* mutant mice. One-way ANOVA, 16 cells for WT, 9 cells for KO, and 16 cells for *Y777H* from three to five mice each (**G**, **H**). Data are presented as mean  $\pm$  SEM. The details of the data are provided in Extended Data Figure 1–1.

BLA glutamatergic neurons in *Slack KO<sup>BL-G-Kcnt1</sup>* mice generated fewer numbers of action potentials than the neurons of the *Slack KO<sup>BL-G-mcherry</sup>* mice in response to the same depolarization current from 30 to 150 pA (Fig. 6R,S; two-way ANOVA with Bonferroni's multiple comparisons test in

S;  $F_{(1,126)} = 42.49$ ,  $p < 0.0001$ ; mCherry group vs *KCNT1* group: –30 pA  $p > 0.9999$ , 0 pA  $p > 0.9999$ , 30 pA  $p = 0.0393$ , 60 pA  $p = 0.0167$ , 90 pA  $p = 0.0167$ , 120 pA  $p < 0.0001$ , 150 pA  $p = 0.0038$ ). Consistent with reduced firing rates, the averaged RP of BLA excitatory neurons of *Slack KO<sup>BL-G-Kcnt1</sup>*



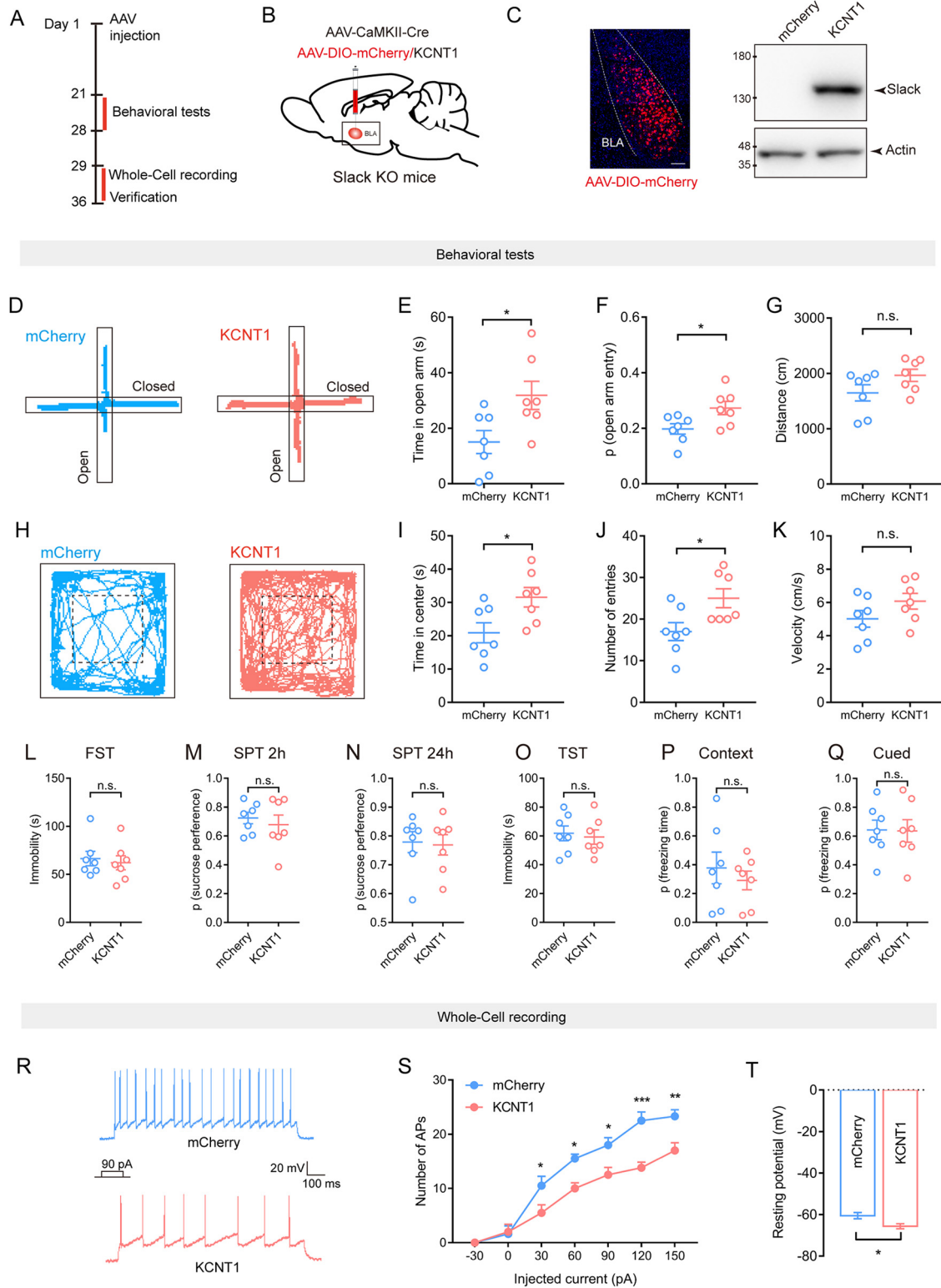


**Figure 6.** Specifically compensatory expression of the Slack channel in BLA glutamatergic neurons rescues the enhanced avoidance behaviors of the *Slack* knock-out mice. **A**, Timeline of AAV injection, behavioral tests, whole-cell recording, scarification, and verification. **B**, Schematic diagram of the specific compensatory expression of the Slack channel in the BLA CaMKII<sup>+</sup> neurons of *Slack* channel knock-out mice. **C**, Left, Confocal images confirmed the mCherry fluorescence specifically expressed in the BLA. Scale bar, 100  $\mu$ m. Right, Western blot confirmation of the Slack channel protein compensatory in the BLA 4 weeks after viral injection. **D–K**, Compensatory expression of the Slack channel in BLA glutamatergic neurons reverses the enhanced avoidance behaviors of *Slack* channel KO mice in EPM (**D–G**) and OF (**H–K**) tests. Representative trajectories of EPM exploration (**D**). Time spent in the anxiogenic open arms (**E**). Probability of open-arm entry (**F**). Total distance traveled in EPM (**G**). Representative trajectories of OF exploration (**H**). Time spent in the anxiogenic center (**I**). Number of entries into the center (**J**). Mice moving velocity (**K**). Two-tailed unpaired *t* test,  $n = 7$ , \* $p < 0.05$  (**E**), \* $p < 0.05$  (**F**), n.s. (**G**), \* $p < 0.05$  (**I**), \* $p < 0.05$  (**J**), n.s. (**K**). **L–Q**, The *Slack* knock-out mice with compensatory expression of the Slack channel in BLA do not exhibit significantly different depressive behavior from the mice with mCherry expression in FST (**L**), SPT 2 h and 24 h (**M**, **N**) and TST (**O**). **P–Q**, Compensated expression of the Slack channel in glutamatergic neurons does not affect contextual fear learning (**P**) or cued fear learning (**Q**). Two-tailed unpaired *t* test,  $n = 7$  (**L–Q**). **R**, Representative traces of action potentials in the BLA CaMKII<sup>+</sup> neurons from Slack KO (mCherry group) and specifically compensatory (*Kcnt1* group) mice in response to 90 pA current pulse lasting for 1 s. Numbers

mice was approximately 5.1 mV lower than the RPs of neurons of the *Slack*  $KO^{BL-G-mCherry}$  mice (Fig. 6T; unpaired *t* test;  $t_{(18)} = 2.655$ ,  $p = 0.0161$ ).

To address the contribution of Slack channel deletion in BLA glutamatergic neurons to anxiety-like behavior, we generated *Slack* channel *CKO* mice by floxing the loxP sites in front of the exon2 and behind the exon32 of the *Kcnt1* gene of mice using CRISPR/Cas9 (clustered regularly interspaced short palindromic repeats/Cas9) technology (Fig. 7A,B). Conditional knock out of the Slack channel in BLA glutamatergic neurons was conducted by injection of AAV-CaMKII-Cre into the *CKO* mice, named  $Kcnt1^{BL-KO}$  mice. *CKO* mice with AAV-CaMKII-mCherry virus injection was used as the control group. (Fig. 7C–E, Extended Data Fig. 7-1A). Successful Slack channels deletion in BLA glutamatergic neurons was validated by qPCR and Western Blot (Fig. 7F,G; unpaired *t* test with Welch's correction in F,  $t_{(3)} = 9.672$ ,  $p = 0.0023$ ; unpaired *t* test in G,  $t_{(6)} = 7.069$ ,  $p = 0.0004$ ). Compared with the control mice,  $Kcnt1^{BL-KO}$  mice spent less time staying and made fewer entries in open arms in the EPM test. Similarly, they made fewer entries to the center and spent less time staying in the center in OF test, whereas no significantly different locomotor activity was observed in both groups of mice (Fig. 7H–O; unpaired *t* test; I,  $t_{(14)} = 2.222$ ,  $p = 0.0433$ ; J,  $t_{(14)} = 2.865$ ,  $p = 0.0125$ ; K,  $t_{(14)} = 0.5254$ ,  $p = 0.6075$ ; M,  $t_{(14)} = 3.113$ ,  $p = 0.0076$ ; N,  $t_{(14)} = 2.614$ ,  $p = 0.0204$ ; O,  $t_{(14)} = 0.02, 0.063$ ,  $p = 0.9838$ ). These findings suggest that Slack channel deletion in BLA glutamatergic neurons is sufficient to cause anxiety in mice.

### Expression of the Slack channel in the BLA–vHPC glutamatergic neurons rescued the enhanced avoidance behaviors of *Slack* *KO* or CORT-treatment mice

To further identify the circuit involved in the Slack channel regulating the avoidance behaviors, we tested the avoidance behaviors after Slack channel expression in the BLA–vHPC glutamatergic inputs in *Slack* *KO* mice (Felix-Ortiz et al., 2013). To generate  $KO^{BL-vHPC-mCherry}$  and  $Slack$   $KO^{BL-vHPC-Kcnt1}$  mice, we injected a mix of AAV2/Retro-CaMKII-Cre and AAV2/9-CaMKII-GFP into the vHPC and Cre-dependent mCherry or *Kcnt1* (AAV-DIO-mcherry/AAV-DIO-*Kcnt1*) into BLA in *Slack* *KO* mice respectively (Fig. 8A,B). Thus, the BLA–vHPC glutamatergic projecting neurons could be labeled by mCherry (Fig. 8C, Extended Data Fig. 7-1B). The  $Slack$   $KO^{BL-vHPC-Kcnt1}$  mice exhibited significantly more exploration time in open arms and entries in open arms in the EPM test than the  $Slack$   $KO^{BL-vHPC-mCherry}$  mice (Fig. 8D–F; unpaired *t* test in E, F; E,  $t_{(10)} = 2.52$ ,  $p = 0.0304$ ; F,  $t_{(10)} = 2.379$ ,  $p = 0.0386$ ). Similarly, the  $Slack$   $KO^{BL-vHPC-Kcnt1}$  mice stayed a longer time in the center and exhibited more entries into the center in the OF test than the  $Slack$   $KO^{BL-vHPC-mCherry}$  mice (Fig. 8H–J; unpaired *t* test in I, J; I,  $t_{(10)} = 2.573$ ,  $p = 0.0277$ ; J,  $t_{(10)} = 2.537$ ,  $p = 0.0295$ ). Data did not show any significant difference in total traveling distances and moving velocity between the two groups of mice (Fig. 8G,K; unpaired *t* test; G,  $t_{(10)} = 0.1409$ ,  $p = 0.8907$ ; K,  $t_{(10)} = 0.08, 4.28$ ,  $p = 0.9345$ ). These results indicated that the enhanced avoidance behaviors of the *Slack* *KO* mice were

abolished by selectively compensating the expression of the Slack channel in BLA–vHPC glutamatergic projection.

To further investigate the role of the Slack channel expressed in BLA–vHPC glutamatergic projection in defending anxiety disorder, we overexpressed the Slack channel in BLA–vHPC glutamatergic projection using the same strategy mentioned above (Fig. 8B). Virus injection was performed 1 d before the beginning of the chronic CORT treatment in naive mice (Fig. 8L,M). Then we examined exploratory behaviors of the mice using EPM and OF tests after 3 weeks of CORT exposure. The Slack overexpressed mice manifested anxiolytic behaviors indicated by staying for a longer time in open arms and more entries into open arms in the EPM test, as well as staying for a longer time in the center and more entries into the center in the OF test than the mCherry control mice (Fig. 8N–U; unpaired *t* test in O–Q, S–U; O,  $t_{(14)} = 2.649$ ,  $p = 0.0191$ ; P,  $t_{(14)} = 2.63$ ,  $p = 0.0198$ ; Q,  $t_{(14)} = 0.5475$ ,  $p = 0.5926$ ; S,  $t_{(14)} = 2.159$ ,  $p = 0.0487$ ; T,  $t_{(14)} = 3.14$ ,  $p = 0.0072$ ; U,  $t_{(14)} = 0.8822$ ,  $p = 0.3926$ ). These findings indicate the role of the Slack channel in BLA–vHPC inputs in preventing pathologic anxiety.

### The expression of the Slack channel in BLA–dmPFC glutamatergic projection neurons does not alter avoidance behaviors or fear memory of the *Slack* *KO* mice

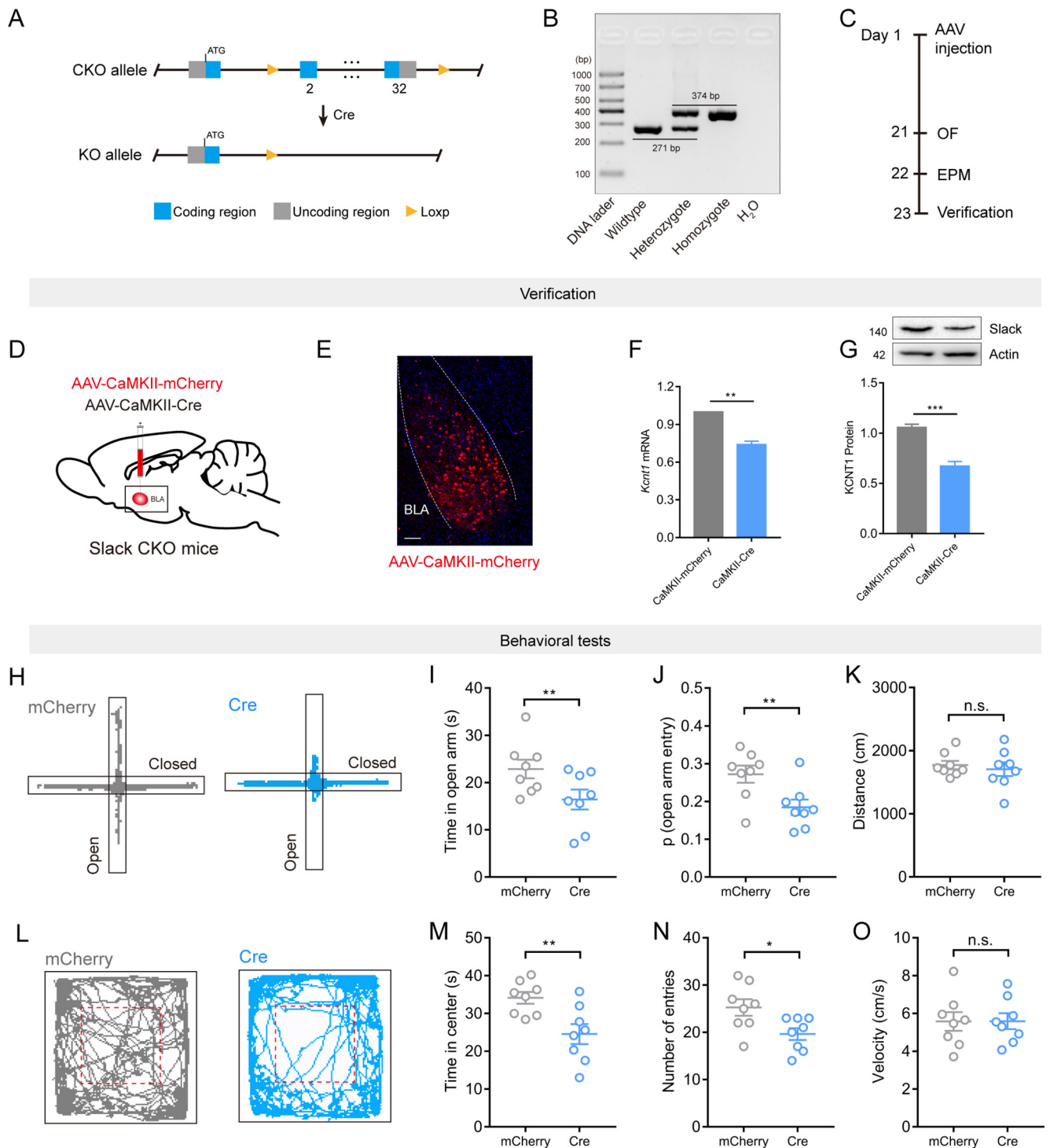
Finally, to distinguish whether the Slack channel only regulates anxiety disorders in a discrete subpopulation of neurons in the BLA, we tested the exploratory and fear behaviors by compensatory expressing the Slack channel in the BLA–dmPFC glutamatergic inputs in *Slack* *KO* mice. Similarly, to generate  $Slack$   $KO^{BL-dmPFC-mCherry}$  and  $Slack$   $KO^{BL-dmPFC-Kcnt1}$  mice, we injected a mix of AAV2/Retro-CaMKII-Cre and AAV2/9-CaMKII-GFP into the dmPFC and Cre-dependent mCherry or *Kcnt1* (AAV-DIO-mCherry/AAV-DIO-*Kcnt1*) into BLA in *Slack* *KO* mice, respectively (Fig. 9A,B). Effective viral expression was verified by the confocal images of GFP and mCherry (Fig. 9C, Extended Data Fig. 7-1C). In contrast to the anxiolytic results of the compensatory expression of the Slack channel in BLA–vHPC glutamatergic inputs in *Slack* *KO* mice, no significant differences were found between  $Slack$   $KO^{BL-dmPFC-mCherry}$  and  $Slack$   $KO^{BL-dmPFC-Kcnt1}$  mice in the EPM (Fig. 9D–G) and OF tests (Fig. 9H–K; unpaired *t* test in E–G, I–K; E,  $t_{(12)} = 0.6582$ ,  $p = 0.5228$ ; F,  $t_{(12)} = 0.3825$ ,  $p = 0.7088$ ; G,  $t_{(12)} = 0.8126$ ,  $p = 0.4323$ ; I,  $t_{(12)} = 0.4327$ ,  $p = 0.6729$ ; J,  $t_{(12)} = 0.519$ ,  $p = 0.6132$ ; K,  $t_{(12)} = 0.3981$ ,  $p = 0.6975$ ). Similarly, no significant differences in fear memory-related behavioral tests were observed between the two groups of mice (Fig. 9L,M; unpaired *t* test; L,  $t_{(10)} = 1.449$ ,  $p = 0.1779$ ; M,  $t_{(10)} = 0.9959$ ,  $p = 0.3428$ ). These data indicate that the Slack channel predominantly regulates anxiety through the BLA subpopulation of glutamatergic neurons projecting to the vHPC but not to the dmPFC.

### Discussion

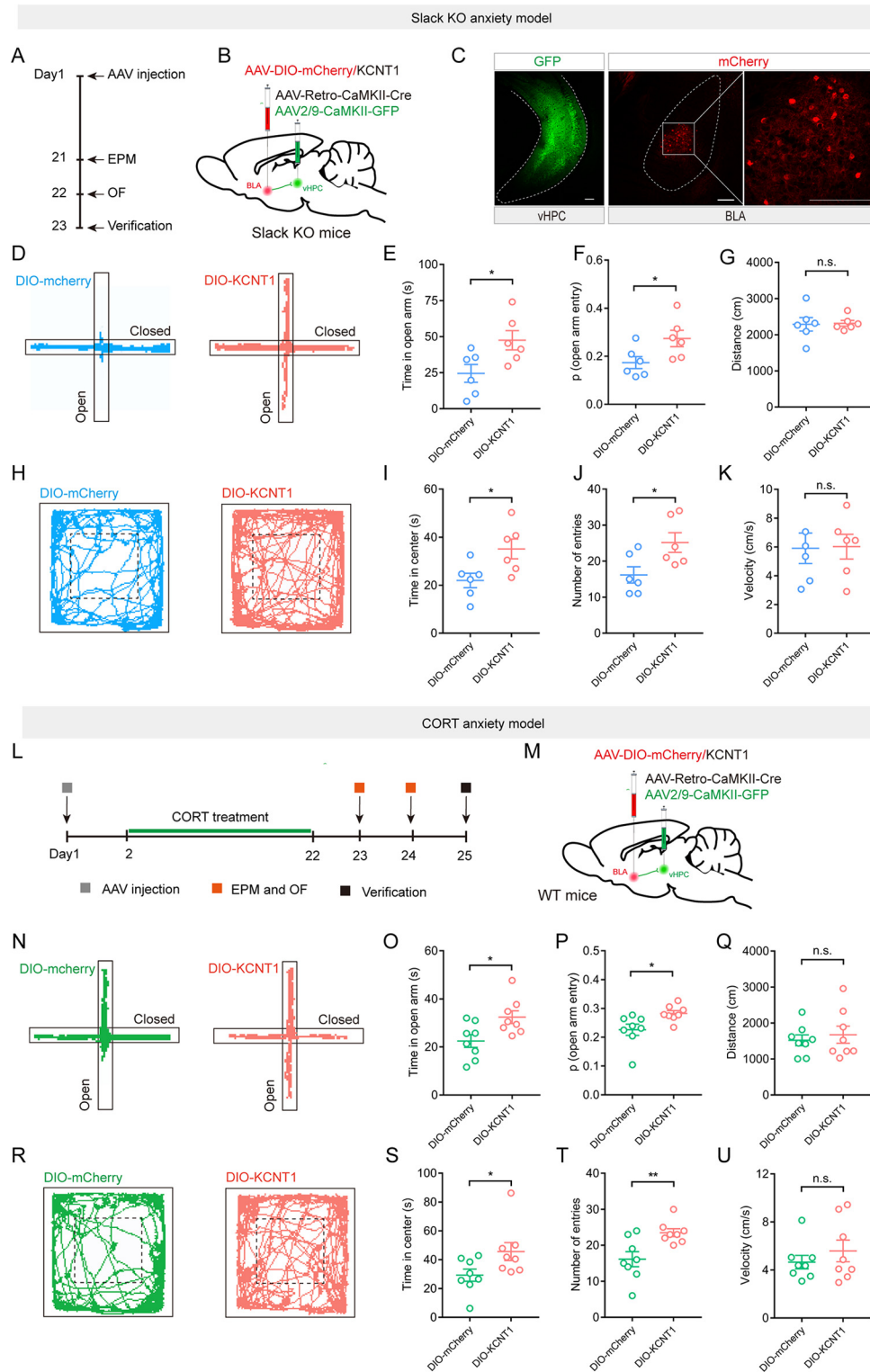
As a prevalent psychiatric disorder, anxiety has been extensively studied. A growing number of studies have focused on the amygdala and its related circuits. However, the contribution of ion channels to the activity of these neuronal circuits and their roles in regulating anxiety behavior is still not well understood. In the present study, we show that the Slack channel is involved in the regulation of anxiety-like behaviors through BLA–vHPC projections (Fig. 10). First, *Slack* *KO* mice exhibit enhanced avoidance behaviors, whereas the Slack gain-of-function mice exhibit reduced avoidance behaviors. Second, Slack channels are richly expressed in BLA glutamatergic neurons and affect the activity of BLA glutamatergic neurons. Third, the compensatory expression

←

of action potentials induced by step current injection (−30 to 150 pA) in the BLA CaMKII+ neurons of the mCherry and *Kcnt1* group mice (5). Data in 5 were analyzed by two-way ANOVA; 10 cells from three to five mice in both groups, \* $p < 0.05$ , \*\* $p < 0.01$ , \*\*\* $p < 0.001$ . Average resting potentials of the BLA CaMKII+ neurons in mCherry and *Kcnt1* group mice (7). Data analyzed by two-tailed unpaired *t* test, 10 cells from three to five mice in both groups, \*\*\* $p < 0.01$ . Data are presented as mean ± SEM. The details of the data are provided in Extended Data Figure 1-1. n.s., Not significant.



**Figure 7.** Conditional knock out of the Slack channel in BLA glutamatergic neurons increases the enhanced avoidance behaviors of the *Slack* CKO mice. **A**, The schematic diagram of the conditional knock-out strategy of the *Kcnt1* gene. **B**, PCR verification of loxp insertion on target gene transcription in *Slack* CKO mice. The 271 bp fragment band is generated from WT alleles, and the 374 bp fragment band is the expected PCR result of the *Slack* CKO genotype. **C**, Timeline of AAV injection, OF and EPM tests, scarification, and verification. **D**, Schematic diagram of injection of AAV-CaMKII-Cre or AAV-CaMKII-mCherry into BLA in *Slack* CKO mice. **E**, Confocal fluorescent images confirm the expression of mCherry the BLA. A schematic of the viral expression for other subjects is provided in Extended Data Figure 7–1A. Scale bar, 100  $\mu$ m. **F**, **G**, Quantification of knock down of Slack channels in mRNA (**F**) and protein levels (**G**) in the BLA of *Slack* CKO mice 3 weeks after AAV-CaMKII-Cre or AAV-CaMKII-mCherry injection. Two-tailed unpaired *t* test,  $n = 4$ ,  $**p < 0.01$  (**F**);  $n = 4$ ,  $***p < 0.001$  (**G**). **H–O**, Conditional knock out of the Slack channel in BLA glutamatergic projection neurons increased avoidance behaviors of mice in the EPM (**H–K**) and OF (**L–O**) test. Representative traces of EPM exploration (**H**). Time spent in the anxiogenic open arms (**I**). Probability of open-arm entry (**J**). Total distance traveled in EPM (**K**). Representative trajectories of OF exploration (**L**). Time spent in the anxiogenic center (**M**). Number of entries into the center (**N**). Moving velocity (**O**). Two-tailed unpaired *t* test;  $n = 8$ ,  $**p < 0.01$  (**I**),  $**p < 0.01$  (**J**), n.s. (**K**),  $**p < 0.01$  (**M**),  $*p < 0.05$  (**N**), n.s. (**O**). Data are presented as mean  $\pm$  SEM. The details of the data are provided in Extended Data Figure 1–1. n.s., Not significant.



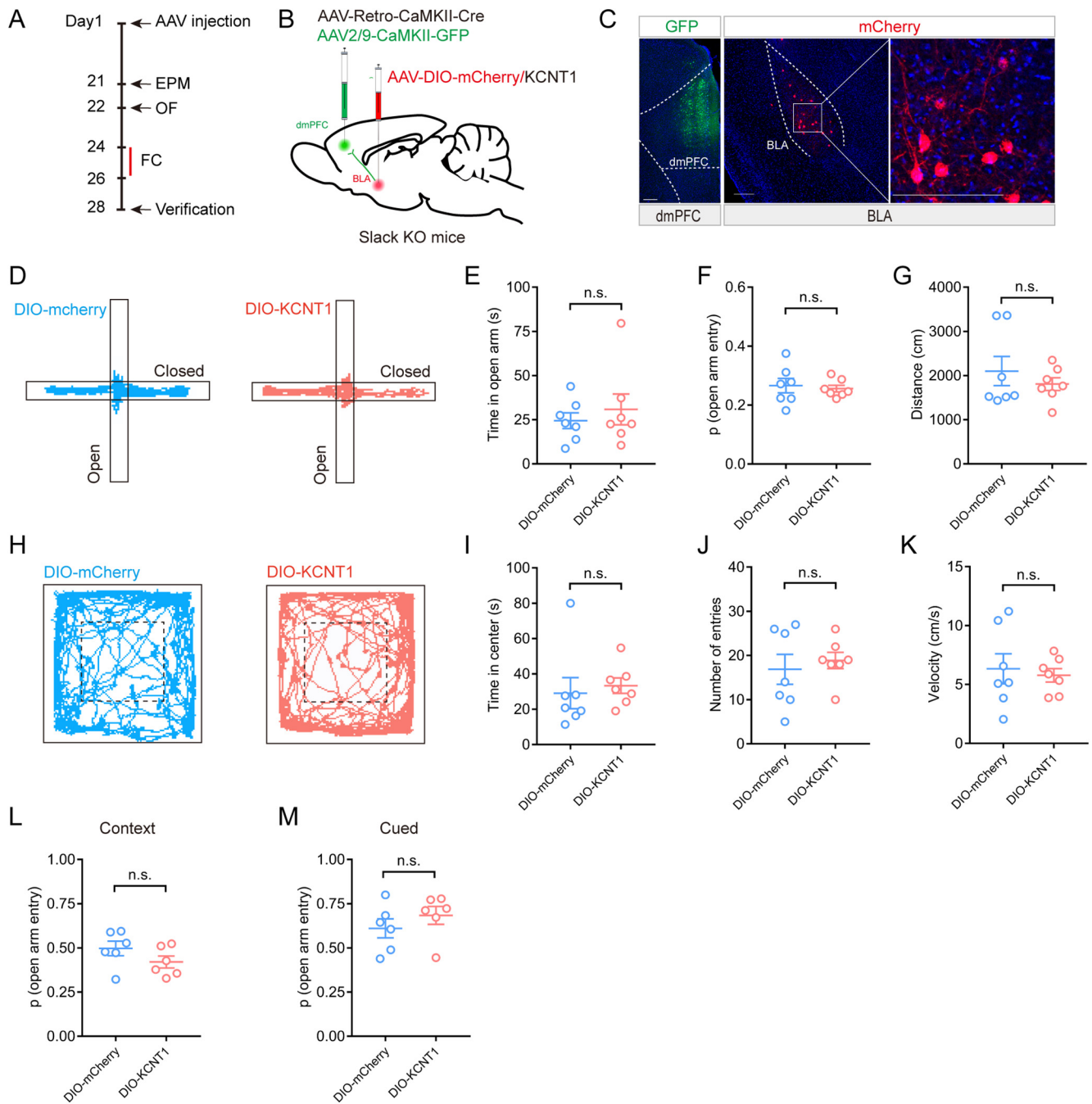


**Figure 9.** The expression of the Slack channel in BLA–dmPFC glutamatergic projection neurons does not alter avoidance behaviors or fear memory of the *Slack KO* mice. **A**, Timeline of AAV injection, avoidance behavioral tests, fear conditioning tests, and verification. **B**, Schematic diagram of injection of AAV-DIO-*Kcnt1* or AAV-DIO-mCherry into BLA and AAV-Retro-CaMKII-Cre mixed with AAV-CaMKII-GFP into dmPFC in *Slack KO* mice. **C**, Confocal fluorescent images confirmed the expression of GFP and mCherry in the dmPFC or BLA, respectively. A schematic of the viral expression for other subjects is provided in Extended Data Figure 7-1C. Scale bar, 200  $\mu$ m. **D–K**, Slack channel expressed in BLA–dmPFC glutamatergic projection neurons does not alter avoidance behaviors of *Slack KO* mice in EPM (**D–G**) and OF (**H–K**) tests. Representative traces of EPM exploration (**D**). Time spent in the anxiogenic open arms (**E**). Probability of open-arm entry (**F**). Total distance traveled in EPM (**G**). Representative trajectories of OF exploration (**H**). Time spent in the anxiogenic center (**I**). Number of entries into the center (**J**). Moving velocity (**K**). **L, M**, Compensate expression of the Slack channel in BLA–dmPFC glutamatergic projection neurons does not affect contextual fear learning (**L**) or cued fear learning (**M**). Two-tailed unpaired *t* test,  $n = 7$ , n.s. (**E–G, I–M**). Data are presented as mean  $\pm$  SEM. The details of the data are provided in Extended Data Figure 1-1. n.s., Not significant.

of the Slack channel in BLA glutamatergic neurons or glutamatergic BLA–vHPC inputs in the *Slack KO* mice abolishes anxious behaviors of *Kcnt1 KO* mice. Fourth, conditional knock out of the Slack channel in BLA glutamatergic neurons also causes enhanced avoidance behaviors. Finally, the Slack channel is specifically downregulated in the BLA of corticosterone-induced anxiety model mice, whereas

overexpression of the Slack channel in BLA of CORT-treated mice prevents the corticosterone-induced anxiety behaviors (Cervantes et al., 2013). These data are sufficient to indicate that the Slack channel plays an essential role in the regulation of anxiety through altering the activity of BLA–vHPC projections despite the wide distribution of the Slack channel in the CNS of mice.

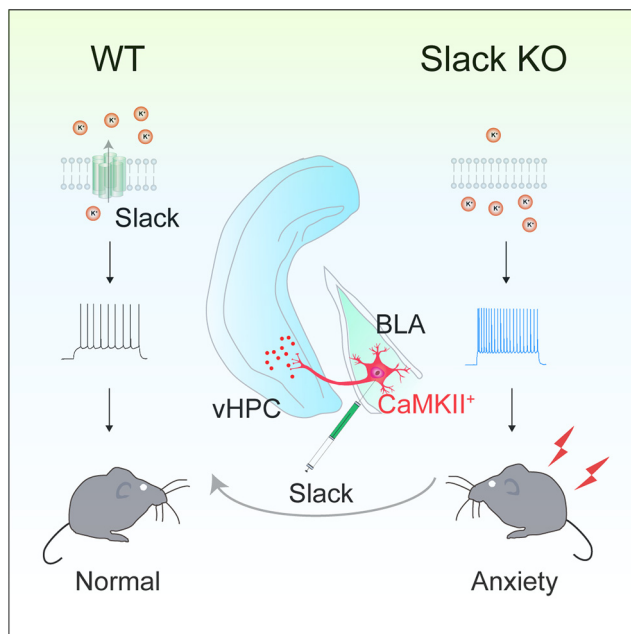


**Figure 10.** Graphical abstract. Schematic showing the role of Slack channels in the regulation of anxiety-like behaviors via basolateral amygdala glutamatergic inputs to the ventral hippocampus.

A previous study observed the enhanced avoidance behaviors in another strain of *Slack* channel KO mice in OF and EPM tests, but the reduced exploration was not attributed to anxiety because of the long initial staying time of the mice in the center of the open field and reduced total travel distance (Bausch et al., 2015). However, we failed to observe the reduced total traveling distance and the long initial staying time in the center of the open field in our *Slack* KO strain (Fig. 1D,H). In addition, conditional Slack channel deletion in BLA also causes enhanced avoidance behaviors (Fig. 7), providing strong evidence to support the attribution of altered exploratory behaviors to anxiety. In addition, the effect of compensatory *Kcnt1* gene expression in the BLA and diazepam administration on suppressing avoidance behaviors argues against the skill-learning defect explanation of the avoidance behaviors (Figs. 1, 4, 6). Interestingly, the antipsychotic drug loxapine, which is a Slack channel activator, is also effective in treating anxiety, but the mechanism has not been addressed (Rickels et al., 1978; Biton et al., 2012). Our results may provide a plausible explanation for the effect. Therefore, our findings identify a new channel mechanism and a potential drug target for the regulation of anxiety.

In addition, the circuit that is involved in chronic cortisone-treatment-induced anxiety has not been clearly defined. A previous study reported a rich expression of glucocorticoid receptors in the amygdala and amygdaloid dendritic hypertrophy caused by cortisone treatment (Mitra and Sapolsky, 2008), indicating the involvement of the amygdala-related circuit in the regulation of cortisone-treatment-induced anxiety. Our findings that *Kcnt1* mRNA and protein expression are downregulated in the BLA, and overexpression of the Slack channel in the BLA–vHPC inputs suppresses the anxiety-like behaviors in CORT-treated mice suggest the involvement of this pathway in the CORT-induced anxiety. Thus, our findings also provide a new circuit and channel mechanism underlying CORT-caused anxiety.

The role of BLA-related neural circuits in the regulation of anxiety is complicated. Although the activation of BLA–vHPC

projection is implicated in anxiogenesis, the activation of pathways from BLA to CeAI (the lateral part of the central amygdala nucleus) and BSTad (the anterodorsal part of the bed nuclei of stria terminalis) result in anxiolytic behaviors (Tye et al., 2011; Kim et al., 2013). The latest research shows that the BLA–vHPC neurons are located in the caudal domain of the anterior BLA (BLA.ac; Hintiryan et al., 2021). Thus, the wide expression of the Slack channel in BLA suggests the possibility that the Slack channel is also involved in other anxiety-related circuits. However, the *Slack* KO mice and *Slack*<sup>BL-KO</sup> mice only demonstrate the anxiogenic effect, indicating a possibility that the role of Slack channel is potent in controlling the activity in subpopulations of neurons projecting from BLA to vHPC but not in other populations of neurons in the BLA. The fear memory, which was controlled by the circuit output from BLA–dmPFC (Tovote et al., 2015; Klavir et al., 2017), was not altered in *Slack* KO mice. Subsequently, compensatory expression of the Slack channel in BLA–dmPFC glutamatergic neurons in the *Slack* KO mice did not alter the fear memory behavior either (Fig. 9). These results support the idea that the Slack channel only potently controls the discrete subpopulation of neurons of BLA–vHPC in the BLA. However, why does the Slack channel not control the BLA–dmPFC circuit to regulate the fear memory? One possibility is that the expression alteration of other ion channels in this circuit produces a compensation mechanism. Another possibility is that the Slack channel deletion alters the activity of more than one circuit that control fear memory. For example, fear memory is also controlled by GABAergic signaling within the basolateral amygdala complex, the anterior cingulate cortex, and ventral hippocampal inputs to the basolateral amygdala (Giachero et al., 2015; Wang et al., 2018; Ortiz et al., 2019). The Slack channel deletion may also alter activities of these circuits to offset the activity alteration in BLA–dmPFC circuit so that the mice did not exhibit obvious fear phenotype. All these speculations need further investigation.

The next question is which potassium channels contribute to controlling the resting potential and activity of BLA neurons in physiological and pathologic conditions. Although alteration of SK (small conductance of potassium) and HCN potassium channel expression in the BLA neurons also affects anxious behaviors (Mitra et al., 2009; Rau et al., 2015; Shao et al., 2019), the absence of direct measurement of the resting potential in the SK or HCN channel knock-out mice limited our understanding of their contribution to BLA neuronal excitabilities. In this study, we found that the absence of Slack channel in BLA glutamatergic neurons elevates their resting potential, increases their firing rates, and consequently increases anxiety-like behaviors in mice (Fig. 5D–H, Fig. 1A–H). In contrast, the gain-of-function Slack channel decreases the resting potential and firing rates of BLA glutamatergic neurons and causes anxiolytic behaviors in mice (Figs. 5D–H, Fig. 2). These data robustly support the contribution of the Slack channel in maintaining the normal excitability of BLA neurons in physiological conditions. However, the Slack channel activity is low in physiological intracellular sodium concentration (2–5 mM). Thus, the high local concentration of sodium is required in maintaining the Slack channel activity, which could be realized by coupling sodium channels activation and the Slack channel opening. The NALCN channel, which is a leaky sodium channel resistant to TTX, is an ideal candidate for coupling the Slack channel activity. The NALCN channel is expressed in the brain (Lu et al., 2007; Ou et al., 2020; Yang et al., 2020), but its expression level in the BLA, especially in the BLA.ac, remains to be explored.

Initially, the *Y777H* mice were constructed for observing the spontaneous epilepsy of mice because this mutant is associated with epilepsy. The *Y777H* mice indeed exhibited high-frequency spontaneous seizures proved by EEG recordings and video monitoring. The seizure frequency is >5 events per week and last 1–20 min with grade 2–3 according to the Racine scale (our unpublished data). But the *Y777H* mice seem to adapt to seizures without increased death rate and other obvious health problems. Thus, we believe the epilepsy phenotype of *Y777H* mice did not influence our anxiety experimental observation. It is noted that sex differences are prominent in anxiety disorders (Altemus et al., 2014), therefore it is a limitation of our study to use only male mice as research subjects in our experiments.

In summary, we report that Slack channels play an essential role in regulating the anxiety-like behaviors in mice via modulating BLA–vHPC glutamatergic neuronal excitability. Our findings shed new light on the ion channel mechanism in anxiety disorders and the molecular basis for the BLA–vHPC circuit in anxiogenic behaviors. We also provide new insights on the neural circuit and ion channel mechanism for the CORT treatment-induced anxiety. The Slack channel is a potential novel pharmacological target in the treatment of anxiety or anxiety-like symptoms in autism, schizophrenia, or other negative emotional diseases.

## References

- Altemus M, Sarvaiya N, Neill Epperson C (2014) Sex differences in anxiety and depression clinical perspectives. *Front Neuroendocrinol* 35:320–330.
- Bausch AE, Dieter R, Nann Y, Hausmann M, Meyerdierks N, Kaczmarek LK, Ruth P, Lukowski R (2015) The sodium-activated potassium channel Slack is required for optimal cognitive flexibility in mice. *Learn Mem* 22:323–335.
- Bhattacharjee A, Gan L, Kaczmarek LK (2002) Localization of the Slack potassium channel in the rat central nervous system. *J Comp Neurol* 454:241–254.
- Biton B, Sethuramanujam S, Picchione KE, Bhattacharjee A, Khessibi N, Chesney F, Lanneau C, Curet O, Avenet P (2012) The antipsychotic drug loxapine is an opener of the sodium-activated potassium channel slack (Slo2.2). *J Pharmacol Exp Ther* 340:706–715.
- Brown MR, Kronengold J, Gazula VR, Chen Y, Strumbos JG, Sigworth FJ, Navaratnam D, Kaczmarek LK (2010) Fragile X mental retardation protein controls gating of the sodium-activated potassium channel Slack. *Nat Neurosci* 13:819–821.
- Carola V, D'Olimpio F, Brunamonti E, Mangia F, Renzi P (2002) Evaluation of the elevated plus-maze and open-field tests for the assessment of anxiety-related behaviour in inbred mice. *Behav Brain Res* 134:49–57.
- Cervantes B, Vega R, Limón A, Soto E (2013) Identity, expression and functional role of the sodium-activated potassium current in vestibular ganglion afferent neurons. *Neuroscience* 240:163–175.
- Dedic N, et al. (2018) Chronic CRH depletion from GABAergic, long-range projection neurons in the extended amygdala reduces dopamine release and increases anxiety. *Nat Neurosci* 21:803–807.
- Evely KM, Pryce KD, Bausch AE, Lukowski R, Ruth P, Haj-Dahmane S, Bhattacharjee A (2017) Slack KNa channels influence dorsal horn synapses and nociceptive behavior. *Mol Pain* 13:1744806917714342.
- Felix-Ortiz AC, Beyeler A, Seo C, Leppla CA, Wildes CP, Tye KM (2013) BLA to vHPC inputs modulate anxiety-related behaviors. *Neuron* 79:658–664.
- Giachero M, Calfa GD, Molina VA (2015) Hippocampal dendritic spines remodeling and fear memory are modulated by GABAergic signaling within the basolateral amygdala complex. *Hippocampus* 25:545–555.
- Gottschalk MG, Domschke K (2017) Genetics of generalized anxiety disorder and related traits. *Dialogues Clin Neurosci* 19:159–168.
- Hintiryan H, et al. (2021) Connectivity characterization of the mouse basolateral amygdala complex. *Nat Commun* 12:2859.
- Howe AS, et al. (2016) Candidate genes in panic disorder: meta-analyses of 23 common variants in major anxiogenic pathways. *Mol Psychiatry* 21:665–679.
- Hu S-W, Zhang Q, Xia S-H, Zhao W-N, Li Q-Z, Yang J-X, An S, Ding H-L, Zhang H, Cao J-L (2021) Contralateral projection of anterior cingulate cortex contributes to mirror-image pain. *J Neurosci* 41:9988–10003.
- Huang CJ, Lin CH, Wu JI, Yang WC (2019) The relationship between depression symptoms and anxiety symptoms during acute ECT for patients with major depressive disorder. *Int J Neuropsychopharmacol* 22:609–615.
- Kim SY, Adhikari A, Lee SY, Marshel JH, Kim CK, Mallory CS, Lo M, Pak S, Mattis J, Lim BK, Malenka RC, Warden MR, Neve R, Tye KM, Deisseroth K (2013) Diverging neural pathways assemble a behavioural state from separate features in anxiety. *Nature* 496:219–223.
- Kjelstrup KG, Tuvnes FA, Steffenach HA, Murison R, Moser EI, Moser MB (2002) Reduced fear expression after lesions of the ventral hippocampus. *Proc Natl Acad Sci U S A* 99:10825–10830.
- Klavriv O, Prigge M, Sarel A, Paz R, Yizhar O (2017) Manipulating fear associations via optogenetic modulation of amygdala inputs to prefrontal cortex. *Nat Neurosci* 20:836–844.
- LeDoux J (2007) The amygdala. *Curr Biol* 17:R868–874.
- Li KX, He M, Ye W, Simms J, Gill M, Xiang X, Jan YN, Jan LY (2019) TMEM16B regulates anxiety-related behavior and GABAergic neuronal signaling in the central lateral amygdala. *Elife* 8:e47106.
- Lu B, Su Y, Das S, Liu J, Xia J, Ren D (2007) The neuronal channel NALCN contributes resting sodium permeability and is required for normal respiratory rhythm. *Cell* 129:371–383.
- Lu R, Bausch AE, Kallenborn-Gerhardt W, Stoetzer C, Debruijn N, Ruth P, Geisslinger G, Leffler A, Lukowski R, Schmidtko A (2015) Slack channels expressed in sensory neurons control neuropathic pain in mice. *J Neurosci* 35:1125–1135.
- Lu S, Das P, Fadool DA, Kaczmarek LK (2010) The slack sodium-activated potassium channel provides a major outward current in olfactory neurons of *Kv1.3*<sup>-/-</sup> super-smeller mice. *J Neurophysiol* 103:3311–3319.
- Mitra R, Sapolsky RM (2008) Acute corticosterone treatment is sufficient to induce anxiety and amygdaloid dendritic hypertrophy. *Proc Natl Acad Sci U S A* 105:5573–5578.
- Mitra R, Ferguson D, Sapolsky RM (2009) SK2 potassium channel overexpression in basolateral amygdala reduces anxiety, stress-induced corticosterone secretion and dendritic arborization. *Mol Psychiatry* 14:847–855, 827.
- Moller RS, et al. (2015) Mutations in *KCNT1* cause a spectrum of focal epilepsies. *Epilepsia* 56:e114–120.
- Mullen SA, Carney PW, Roten A, Ching M, Lightfoot PA, Churilov L, Nair U, Li M, Berkovic SF, Petrou S, Scheffer IE (2018) Precision therapy for epilepsy due to *KCNT1* mutations: a randomized trial of oral quinidine. *Neurology* 90:e67–e72.
- Ortiz S, Latsko MS, Fouty JL, Dutta S, Adkins JM, Jasnow AM (2019) Anterior cingulate cortex and ventral hippocampal inputs to the basolateral amygdala selectively control generalized fear. *J Neurosci* 39:6526–6539.
- Ou M, Zhao W, Liu J, Liang P, Huang H, Yu H, Zhu T, Zhou C (2020) The general anesthetic isoflurane bilaterally modulates neuronal excitability. *iScience* 23:100760.
- Pan Z, Zhang Q, Liu X, Zhou H, Jin T, Hao L-Y, Xie L, Zhang M, Yang X-X, Sun M-L, Xue Z-Y, Tao Y, Ye X-C, Shen W, Cao J-L (2021) *Mettl3* contributes to inflammatory pain by targeting TET1 in YTHDF2-dependent manner. *Pain* 162:1960–1976.
- Park K, Yi JH, Kim H, Choi K, Kang SJ, Shin KS (2011) HCN channel activity-dependent modulation of inhibitory synaptic transmission in the rat basolateral amygdala. *Biochem Biophys Res Commun* 404:952–957.
- Peng B, Xu Q, Liu J, Guo S, Borgland SL, Liu S (2021) Corticosterone attenuates reward-seeking behavior and increases anxiety via D2 receptor signaling in ventral tegmental area dopamine neurons. *J Neurosci* 41:1566–1581.
- Pidoplichko VI, Aroniadou-Anderjaska V, Prager EM, Figueiredo TH, Almeida-Suhett CP, Miller SL, Braga MF (2014) ASIC1a activation enhances inhibition in the basolateral amygdala and reduces anxiety. *J Neurosci* 34:3130–3141.
- Rau AR, Chappell AM, Butler TR, Ariwodola OJ, Weiner JL (2015) Increased basolateral amygdala pyramidal cell excitability may contribute to the anxiogenic phenotype induced by chronic early-life stress. *J Neurosci* 35:9730–9740.

- Rickels K, Weise CC, Feldman H, Fee EA, Wiswesser G (1978) Loxapine in neurotic anxiety: some modifiers of treatment response. *J Int Med Res* 6:180–185.
- Rizzi S, Knaus HG, Schwarzer C (2016) Differential distribution of the sodium-activated potassium channels *slack* and *slick* in mouse brain. *J Comp Neurol* 524:2093–2116.
- Salimando GJ, Hyun M, Boyt KM, Winder DG (2020) BNST GluN2D-containing NMDA receptors influence anxiety- and depressive-like behaviors and modulate cell-specific excitatory/inhibitory synaptic balance. *J Neurosci* 40:3949–3968.
- Shao LX, Jiang Q, Liu XX, Gong DM, Yin YX, Wu G, Sun NH, Wang CK, Chen QZ, Yu C, Shi WX, Fan HY, Fukunaga K, Chen Z, Lu YM, Han F (2019) Functional coupling of *Tmem74* and *HCN1* channels regulates anxiety-like behavior in BLA neurons. *Mol Psychiatry* 24:1461–1477.
- Tang QY, Zhang FF, Xu J, Wang R, Chen J, Logothetis DE, Zhang Z (2016) Epilepsy-related *Slack* channel mutants lead to channel over-activity by two different mechanisms. *Cell Rep* 14:129–139.
- Tovote P, Fadok JP, Lüthi A (2015) Neuronal circuits for fear and anxiety. *Nat Rev Neurosci* 16:317–331.
- Tye KM, Prakash R, Kim SY, Fenno LE, Grosenick L, Zarabi H, Thompson KR, Gradinaru V, Ramakrishnan C, Deisseroth K (2011) Amygdala circuitry mediating reversible and bidirectional control of anxiety. *Nature* 471:358–362.
- Wang Q, Wang Q, Song XL, Jiang Q, Wu YJ, Li Y, Yuan TF, Zhang S, Xu NJ, Zhu MX, Li WG, Xu TL (2018) Fear extinction requires *ASIC1a*-dependent regulation of hippocampal-prefrontal correlates. *Sci Adv* 4:eaau3075.
- Xia SH, Hu SW, Ge DG, Liu D, Wang D, Zhang S, Zhang Q, Yuan L, Li YQ, Yang JX, Wu P, Zhang H, Han MH, Ding HL, Cao JL (2020) Chronic pain impairs memory formation via disruption of neurogenesis mediated by mesohippocampal brain-derived neurotrophic factor signaling. *Biol Psychiatry* 88:597–610.
- Yang Y, Ou M, Liu J, Zhao W, Zhuoma L, Liang Y, Zhu T, Mulkey DK, Zhou C (2020) Volatile anesthetics activate a leak sodium conductance in retrotrapezoid nucleus neurons to maintain breathing during anesthesia in mice. *Anesthesiology* 133:824–838.
- Yuan A, Santi CM, Wei A, Wang ZW, Pollak K, Nonet M, Kaczmarek L, Crowder CM, Salkoff L (2003) The sodium-activated potassium channel is encoded by a member of the *Slo* gene family. *Neuron* 37:765–773.
- Zhang WH, Liu WZ, He Y, You WJ, Zhang JY, Xu H, Tian XL, Li BM, Mei L, Holmes A, Pan BX (2019) Chronic stress causes projection-specific adaptation of amygdala neurons via small-conductance calcium-activated potassium channel downregulation. *Biol Psychiatry* 85:812–828.
- Zhang Y, Brown MR, Hyland C, Chen Y, Kronengold J, Fleming MR, Kohn AB, Moroz LL, Kaczmarek LK (2012) Regulation of neuronal excitability by interaction of fragile X mental retardation protein with *slack* potassium channels. *J Neurosci* 32:15318–15327.
- Zhang Z, Rosenhouse-Dantsker A, Tang QY, Noskov S, Logothetis DE (2010) The *RCK2* domain uses a coordination site present in *Kir* channels to confer sodium sensitivity to *Slo2.2* channels. *J Neurosci* 30:7554–7562.